1307

NOVEMBER 1976 PPPL-1307

LOWER HYBRID PARAMETRIC INSTABILITIES - SATURATION BY CASCADING AND PUMP DEPLETION

BY

R. L. BERGER, LIU CHEN, AND
F. W. PERKINS

PLASMA PHYSICS LABORATORY

MASTER

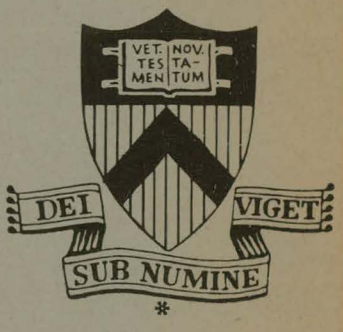

DISTRIBUTION OF THIS DOCUMENT IS UNLIMITED

PRINCETON UNIVERSITY
PRINCETON, NEW JERSEY

This work was supported by U. S. Energy Research and Development Administration Contract E(11-1)-3073. Reproduction, translation, publication, use and disposal, in whole or in part, by or for the United States Government is permitted.

DISCLAIMER

This report was prepared as an account of work sponsored by an agency of the United States Government. Neither the United States Government nor any agency Thereof, nor any of their employees, makes any warranty, express or implied, or assumes any legal liability or responsibility for the accuracy, completeness, or usefulness of any information, apparatus, product, or process disclosed, or represents that its use would not infringe privately owned rights. Reference herein to any specific commercial product, process, or service by trade name, trademark, manufacturer, or otherwise does not necessarily constitute or imply its endorsement, recommendation, or favoring by the United States Government or any agency thereof. The views and opinions of authors expressed herein do not necessarily state or reflect those of the United States Government or any agency thereof.

DISCLAIMER

Portions of this document may be illegible in electronic image products. Images are produced from the best available original document.

NOTICE

This report was prepared as an account of work sponsored by the United States Government. Neither the United States nor the United States Energy Research and Development Administration, nor any of their employees, nor any of their contractors, subcontractors, or their employees, makes any warranty, express or implied, or assumes any legal liability or responsibility for the accuracy, completeness or usefulness of any information, apparatus, product or process disclosed, or represents that its use would not infringe privately owned rights.

Printed in the United States of America.

Available from
National Technical Information Service
U. S. Department of Commerce
5285 Port Royal Road
Springfield, Virginia 22151
Price: Printed Copy $ * ; Microfiche $3.00

*Pages	NTIS Selling Price
1-50	$ 4.00
51-150	5.45
151-325	7.60
326-500	10.60
501-1000	13.60

Lower Hybrid Parametric Instabilities - Saturation by Cascading and Pump Depletion

R. L. Berger, Liu Chen, and F. W. Perkins

Plasma Physics Laboratory, Princeton University
Princeton, New Jersey 08540

November 1976

PPPL-1307

NOTICE

This report was prepared as an account of work sponsored by the United States Government. Neither the United States nor the United States Energy Research and Development Administration, nor any of their employees, nor any of their contractors, subcontractors, or their employees, makes any warranty, express or implied, or assumes any legal liability or responsibility for the accuracy, completeness or usefulness of any information, apparatus, product or process disclosed, or represents that its use would not infringe privately owned rights.

MASTER

DISTRIBUTION OF THIS DOCUMENT IS UNLIMITED

Lower Hybrid Parametric Instabilities - Saturation by Cascading and Pump Depletion

R. L. Berger, Liu Chen, F. W. Perkins
Plasma Physics Laboratory, Princeton University
Princeton, New Jersey 08540

ABSTRACT

Parametric instabilities near the lower hybrid frequency and associated electron and ion heating have been observed experimentally for some years, most recently in radio-frequency heating experiments on the Adiabatic Toroidal Compressor Tokamak. Here, the nonlinear evolution and saturation by cascading of the parametric decay instability near the lower hybrid frequency is considered by solving a weak-turbulence wave kinetic equation. The principal results are that 1) a steady state solution exists only for pumps near threshold when the pump frequency is several times the lower hybrid frequency; 2) the decay instability saturates when the energy in decay waves is roughly equal to the pump energy; 3) most of the pump energy is deposited in super thermal electrons when $\omega_o >> \omega_{\ell h}$ and 4) pump depletion in the low-density surface plasma will be a serious problem unless the pump power is kept near threshold for large tokamaks.

I. INTRODUCTION

Heating of plasma by conversion of wave energy to thermal energy is one of the primary means under consideration to raise the plasma temperature to the thermonuclear range. A particularly interesting and convenient method is lower hybrid frequency heating[1] because, for tokamak plasmas, the frequency of the radiation is such that the waves can be introduced by arrays of waveguides. Each waveguide array is arranged so that the electric field vector in each waveguide is phased properly so as to meet accessibility criteria.[2] Unless a large number of waveguide arrays are employed, the heating of both reactor and research tokamaks will require power levels in each array that will surely exceed the thresholds for nonlinear effects such as parametric instabilities.[3] That nonlinear effects appear to play the dominant role in radio frequency heating near the lower hybrid frequency has been shown by simultaneous appearance of decay wave spectra and high-energy tails on the electron and ion velocity distribution.[4] The ion and electron heating has been measured in small devices by ion and electron energy analyzers and in the Adiabatic Toroidal Compressor Tokamak by fast neutrals and synchrotron radiation.[5]

The parametric instabilities of primary interest to lower hybrid heating are decay of the incident electrostatic wave into lower frequency lower hybrid waves by scattering off the ion and electron distribution and the oscillating two stream instability (OTSI). Filamentation instabilities[6,7] have a much higher threshold than these. In hot nonuniform plasmas such as tokamaks, both 'uniform' medium and convective quasimode thresholds are exceeded.

The threshold for convective quasimode decay has been shown to be determined by the finite spatial extent of the pump wave while the 'uniform' medium threshold pertains to waves ducted by the density profile;and hence destabilized by the spatially averaged field. The impressed lower hybrid pump waves, launched by wave-quides or other finite structures at the plasma boundary, are known to propagate such that the energy of the wave is confined to a good approximation within well-defined resonance cones.[8] As a result, the thresholds of convective quasimode instabilities are determined by the loss of the wave out of the resonance cone (the amplifying medium) balancing the growth of the wave due to transfer of energy from the pump wave. As a result of these considerations, it has been shown that the dominant parametric instabilities are nonlinear Landau damping of lower hybrid waves and oscillating two streaming instability

Examination of the threshold formula for parametric decay instabilities shows that the instabilities are most likely to occur in the cold, low-density periphery region where $\omega_o >> \omega_{\ell h}$ and in the plasma interior where $\omega_o \lesssim 2\omega_{\ell h}$. Furthermore, the lower hybrid waves destabilized by the oscillating two stream instability are nearly identical to those created by the decay instability, and hence subject to the same saturation mechanisms. Therefore, we have investigated the nonlinear saturation of the decay instability by cascading for pump frequencies in the range one to four times the lower hybrid frequency. We chose the electron to ion temperature ratio equal to one which is typical of tokamaks, and thus the low-frequency wave is a nonresonant

quasi-mode. As a consequence, wave energy is not conserved in the decay process; however, action $I_{\underset{\sim}{k}}$ is conserved and a small amount of wave energy is dissipated in the scattering process. Two questions that we seek to answer are 1) under what conditions is the cascading model adequate to saturate the decay instability and 2) how much energy relative to the pump energy is in decay waves at saturation and what is the anomalous damping rate for the pump? We find that the model is only adequate to saturate decay instabilities near threshold. For pump powers less than several times the threshold power, we find the anomalous damping rate γ_{eff} is proportional to the pump power Π relative to threshold power Π_{TH} times the typical damping rate $\bar{\gamma}$ of the decay waves, i.e. $\gamma_{eff} = \alpha\bar{\gamma}\Pi/\Pi_{TH}$. We have estimated the scale length for pump depletion in typical tokamaks and found that the pump wave should be able to penetrate to the plasma interior even when the pump power is several times threshold for current tokamak heating experiments. However, future experiments present a problem because the amount of pump depletion scales linearly with plasma size. Once the pump penetrates to the plasma interior, the pump power will be many times threshold, a condensation phenomena occurs,[9] and our model becomes inadequate to predict the saturated state of plasma turbulence. But from the viewpoint of tokamak heating, the really crucial question is not what the details of nonlinear absorption in the plasma interior are, but whether most of the power will be absorbed in the outer regions. Hence, our principal concern lies with the low-density region $\omega_o >> \omega_{\ell h}$ and the non-

linear Landau damping cascade model is valid for a good range of powers.

The paper is organized as follows: Section II presents the basic equations describing the parametric interaction of lower hybrid waves via nonlinear Landau damping, derives some conservation laws, and gives an estimate of the saturated level of turbulence. Section III presents the results of a numerical solution of the wave kinetic equation derived in Sec. II The scaling law is obtained for the total energy in decay waves in steady state versus the pump power. Section IV shows how the nonlinear pump depletion scale length varies with plasma size and parallel wavelength of the pump. Section V discusses the implications of the previous sections to tokamak heating.

II. BASIC EQUATIONS AND ASSUMPTIONS

The process we seek to describe is the nonlinear evolution and saturation by cascading of the parametric decay instability near the lower hybrid frequency. Other mechanisms for saturation of the decay instability exist such as quasilinear modification of the velocity distribution, beat wave trapping, orbit diffusion, and pump depletion. In general, these processes are important for pump powers far above threshold. We are interested in pumps near threshold where characteristically

$$|E_{o\perp}|^2 \simeq (T_e/m_i c^2) B_o^2 \quad \text{or} \quad \frac{E_o^2}{4\pi n T_e} \simeq \left(\frac{m_e}{m_i}\right) \frac{\omega_{ce}^2}{\omega_{pe}^2} << 1 \quad . \qquad (1)$$

Inequality (1) holds except at very low-densities near the vessel wall. The total energy in high-frequency decay waves when saturation by cascading occurs is typically equal to the pump energy. The energy in the beat wave is smaller than this by the ratio $(\omega_o - \omega_k)/\omega_o$ and thus, is not sufficient to flatten the distribution near the thermal velocity. Moreover the large conductivity of electrons along the field line and of the ions across the field lines will inhibit plateau formation since the parametric interaction is in fact localized in space. Pump depletion will be discussed in Sec. III. Trapping becomes important when the amplitude of oscillation of the particle in the potential of the decay wave nears the phase velocity. Since the dominant electric field induces an electron oscillation perpendicular to the phase velocity, it is clearly unimportant for electrons. For ions this requires

$$\frac{ek^2\phi_k}{m_i\omega_k^2} \sim 1 \quad \text{or} \quad \frac{|E_k|^2}{4\pi nT_e} \simeq \frac{\omega_k^2}{\omega_{pi}^2}\left(\frac{\omega_k^2}{k^2v_i^2}\right) > 1 ,$$

which is far above the level for which cascading is important. For the same reason, we feel that orbit diffusion is unimportant.

At frequencies near the lower hybrid frequency, $\omega << \omega_{ce}$, ω_{pe} , the dominant coupling between waves results from the drift of the electrons relative to the ions due to the $\underset{\sim}{E} \times \underset{\sim}{B}_o$ drift of the electrons across the field lines coupling with the nonresonant low-frequency density perturbation produced at the beat frequency of the two lower hybrid waves. The transfer of wave energy from the pump to the decay waves and from one decay wave to another takes place via nonlinear Landau damping. This nonresonant process is the dominant one when resonant decay instabilities are suppressed either by geometrical effects, violation of the selection rules, or restrictions on the volume of wavenumber space available. It has been shown that the threshold is determined by the fact that the high-frequency daughter wave convects out of the resonance cone of the pump wave in a transit time. The transit time, τ_{TR}, equal to the width of the cone projected along the direction of the group velocity divided by the group velocity magnitude, must be long compared to a growth time τ_g in order for significant growth to occur, i.e., $\tau_{TR} > \tau_g$. Since the transit time is proportional to wavenumber for lower hybrid waves, any low-frequency response that occurs for wavelengths short compared to an ion gyroradius will allow the maximum growth of the lower hybrid daughter wave

provided $k\lambda_D$ is not so large that the daughter wave is severely Landau damped (typically $k\lambda_D \lesssim 0.25$). Because $\lambda_{De} << r_i$, the ion-Larmor radius, for physically interesting plasmas, coupling to ion-acoustic waves ($|\omega| >> \omega_{ci}$, $kr_i >> 1$) or nonlinear Landau damping if $T_e \sim T_i$ appears to be the most interesting nonlinear process.

In the rest of this paper, we limit our consideration to nonlinear Landau damping or quasimode decay. We assume that the electrons are magnetized and that $k^2 r_e^2 << 1$ where r_e is the electron-Larmor radius. Thus, the electron susceptibility at the beat frequency is

$$\chi_e(k,\omega) = (1/k^2\lambda_{De}^2)\ W(\omega/\sqrt{2}\ k_{||}\ v_e) \ ,$$

where $W(\xi) = [1 + \xi Z(\xi)]$ and $Z(\xi)$ is the plasma dispersion function. We assume that the ions are unmagnetized and that $k^2 r_i^2 >> 1$. Thus, the ion susceptibility at the beat frequency is

$$\chi_i(k,\omega) = W(\omega/\sqrt{2}\ k_\perp v_i)/k^2\lambda_{Di}^2 \ . \qquad (2)$$

This approximation is clearly justified for the real part of the susceptibility. The imaginary part is also correct if the growth rate is large compared to the ion-cyclotron frequency or if the bandwidth of the lower hybrid waves is large compared to ω_{ci} but small compared to kc_s. In practice $\omega_{pe} \simeq \omega_{ce}$ and a bandwidth, $\Delta\omega = \omega_{ci}$, is a small fraction of the lower hybrid wave frequency, i.e., $\Delta\omega/\omega \sim \omega_{ci}/\omega_{pi} \sim (m_e/m_i)^{1/2}$.

If $T_e > 3T_i$ and $k_{||}/k >> (m_e/m_i)^{1/2}$, the low-frequency response can be expressed analytically by the approximate formulae

$$\chi_e = \frac{1}{k^2\lambda_{De}^2}\left(1 + \frac{i\omega\sqrt{\pi}}{\sqrt{2}\,k_{||}\,v_e}\right), \quad \chi_i = -\frac{\omega_{pi}^2}{\omega^2}\left(1 + \frac{3k^2v_i^2}{\omega^2}\right)$$

$$+ \frac{i}{k^2\lambda_{Di}^2}\,\frac{\sqrt{\pi}}{\sqrt{2}}\,\frac{\omega}{kv_i}\exp\left(-\frac{\omega^2}{2k^2W_i^2}\right),$$

where $v_i = (T_i/m_i)^{1/2}$ and $v_e = (T_e/m_e)^{1/2}$. In this limit the low-frequency response is resonant, $\mathrm{Re}\,\varepsilon(k,\omega) = 0$, and maximum coupling obtains when $\omega = \omega_A + i\gamma_A$ where $\omega_A = kc_s$,

$$\gamma_A = \frac{\omega_A}{2\sqrt{2}}\left(1 + \frac{3T_i}{T_e}\right)^{1/2}\left[\frac{k}{k_{||}}\left(\frac{m_e}{m_i}\right)^{1/2} + \left(\frac{T_e}{T_i}\right)^{3/2}\exp\left(-\frac{c_s^2}{2v_i^2}\right)\right]$$

and

$$c_s = [(T_e + 3T_i)/m_i]^{1/2}.$$

If $T_e \lesssim 3T_i$, then the real part of the dielectric doesn't vanish for any value of ω. However, the maximum response for $k_{||}/k > (m_e/m_i)^{1/2}$ still occurs when $\mathrm{Re}\,\omega = kc_s$. In this case, the low-frequency response is dissipative because the beat phase velocity is close to the ion thermal velocity if $k_{||}/k >> (m_e/m_i)^{1/2}$ or to the electron thermal velocity if $k_{||}/k \sim (m_e/m_i)^{1/2}$.

Because the beat wave is a highly damped wave, i.e. $\gamma_A \sim \omega_A >> \gamma$, where γ is the parametric growth role, the low frequency wave amplitude is related to the amplitude of the high frequency wave by its linear properties. The low frequency response can, therefore, be obtained by introducing a nonlinear ponderomotive potential produced by the beating of two high frequency waves into the Vlasov-Maxwell equations for the low frequency response with the result that

$$4\pi e n^L(\underset{\sim}{k},\omega) = -\frac{ic}{B_o} k^2 \frac{1 + \chi_i(\underset{\sim}{k},\omega)}{\varepsilon(\underset{\sim}{k},\omega)} \int d^3\underset{\sim}{k}' \int d\omega' \, (\underset{\sim}{k}' \times \hat{e}_z)\cdot\underset{\sim}{k} \, \phi(\underset{\sim}{k}',\omega')$$

$$\phi(\underset{\sim}{k}-\underset{\sim}{k}', \omega-\omega') \left(\frac{k_{\parallel} - k_{\parallel}'}{\omega-\omega'} - \frac{k_{\parallel}'}{\omega'} \right) \quad . \tag{3}$$

This result is combined with the equation for the high frequency wave potential

$$\left(\frac{\partial^2}{\partial t} + \omega_k^2 + 2\frac{\partial}{\partial t}\gamma_k\right)\phi_k = -\frac{4\pi ec}{k^2 B_o} \frac{\partial}{\partial t} \int d^3\underset{\sim}{k}' \, \phi(\underset{\sim}{k}',t) n^L(\underset{\sim}{k}-\underset{\sim}{k}',t)$$

$$\underset{\sim}{k}\cdot(\hat{e}_z \times \underset{\sim}{k}') \, , \tag{4}$$

to obtain a nonlinear coupled mode equation. If the random phase approximation, i.e. $\langle \phi_{\underset{\sim}{k}} \phi^*_{\underset{\sim}{k}'} \rangle = \mathcal{E}_{\underset{\sim}{k}} \delta_{\underset{\sim}{k},\underset{\sim}{k}'}$, is valid the nonlinear evolution of the parametrically unstable lower hybrid waves can be described by a wave kinetic equation[10]

$$\frac{1}{2}\frac{\partial}{\partial t} I_{\underset{\sim}{k}} = (\gamma_L + \gamma^0_{\underset{\sim}{k}} + \gamma^{NL}_{\underset{\sim}{k}}) I_{\underset{\sim}{k}} + S_{\underset{\sim}{k}} \, , \tag{5}$$

where $I_{\underset{\sim}{k}}$ is the wave action or number density, γ_L is the sum of all linear losses, $\gamma^{\circ}_{\underset{\sim}{k}}$ is the growth rate of the mode due to nonlinear Landau damping of the pump, $\gamma^{NL}_{\underset{\sim}{k}}$ is the growth rate due to the nonlinear Landau damping of the decay waves, and $S_{\underset{\sim}{k}}$ is the spontaneous emission of lower hybrid waves which is dominated by the low-frequency noise beating with the pump and excited decay waves to produce a source at high-frequencies.[11] A derivation of the spontaneous emission term is given in the Appendix. The definition of these quantities is

$$I_{\underset{\sim}{k}} = \frac{k^2 |\phi_k|^2}{4\pi} \frac{(1+\omega_{pe}^2/\omega_{ce}^2)}{(2\pi)^3 \omega_k} , \tag{6}$$

$$\gamma^{\circ}_{\underset{\sim}{k}} = -\frac{c^2}{8B_o^2 C_s^2} \frac{\omega_{\ell h}^2}{\omega_o^2} \left| \frac{\underset{\sim}{k} \times \underset{\sim}{E}_o}{k} \right|^2 B(\underset{\sim}{k}, \omega_k - \omega_o)\ \omega_k \tag{7}$$

$$\gamma_L = \gamma^* + \frac{1}{2}\left(\frac{\pi}{2}\right)^{1/2} \frac{\omega_{\ell h}^2}{\omega_{\underset{\sim}{k}}} \frac{\omega_k^2}{k_\perp^2 v_i^2} \left[\frac{\omega_k}{k_\perp v_i} \exp\left(-\frac{\omega_k^2}{2k_\perp^2 v_i^2}\right) \right. \tag{8}$$

$$\left. + \frac{T_i}{T_e} \frac{\omega_k}{k_{||} v_e} \exp\left(-\frac{\omega_k^2}{2k_{||}^2 v_e^2}\right) \right] + \frac{\nu_e}{2}\left(\frac{\omega_{pe}^2}{\omega_{pe}^2+\omega_{ce}^2} + \frac{\omega_k^2 - \omega_{\ell h}^2}{\omega_k^2}\right) ,$$

$$\gamma_{NL} = -\frac{4\pi c^2 \omega_{\ell h}^2}{2B_o^2 C_s^2 (1+\omega_{pe}^2/\omega_{ce}^2)} \int d^3\underset{\sim}{k}' \frac{(\underset{\sim}{k}\times\underset{\sim}{k}'\cdot\underset{\sim}{z})^2}{k^2 k'^2} B(\underset{\sim}{k}'-\underset{\sim}{k}\ ,\ \omega_{\underset{\sim}{k}'} - \omega_{\underset{\sim}{k}}) I_{\underset{\sim}{k}'} \tag{9}$$

$$S_{\underset{\sim}{k}} = (2\pi)^{-6}\left(\frac{\pi}{2}\right)^{1/2} \frac{T_e}{16\pi} \frac{c^2 \left|\underset{\sim}{k}_\perp \times \underset{\sim}{E}_{o\perp}\right|^2}{B_o^2 C_s^2 k^2} \frac{\omega_{\ell h}}{\omega_k} \chi\, G(\underset{\sim}{k}, \omega_k = \omega_o)$$

$$+\left(\frac{\pi}{2}\right)^{1/2} \frac{4\pi\, T_e}{(1+\omega_{pe}^2/\omega_{ce}^2)} \frac{c^2}{B_o^2 C_s^2} \int \frac{d^3\underset{\sim}{k}'}{(2\pi)^3} \frac{\left[(\underset{\sim}{k}\times\underset{\sim}{k}')\cdot\hat{\underset{\sim}{z}}\right]^2}{k^2 k'^2} I_{\underset{\sim}{k}'} G(\underset{\sim}{k}-\underset{\sim}{k}',\ \omega_{\underset{\sim}{k}}-\omega_{\underset{\sim}{k}'})$$

where

$$G(k,\omega) = \frac{T_e^2}{T_i^2}\left|\frac{W_i}{k^2\lambda_{De}^2 + W_e + \frac{T_e}{T_i}W_i}\right|^2 \frac{\omega_{\ell h}}{|k_{||}|v_e}$$

$$\chi\left[\exp\left(-\frac{\omega^2}{2k_{||}^2 v_e^2}\right) + \left(\frac{m_i}{m_e}\right)^{1/2}\frac{k_{||}}{k}\left(\frac{T_e}{T_i}\right)^{1/2}\exp\left(-\frac{\omega^2}{2k^2 v_i^2}\right)\right]$$

and

$$B(k,\omega) = \mathrm{Im}\left(\frac{T_e}{T_i}\frac{W_e W_i}{k^2\lambda_{De}^2 + W_e + T_e W_i/T_i}\right), \tag{10}$$

and $W_e = W(\omega/\sqrt{2}k_{||}v_e)$, $W_i = W(\omega/\sqrt{2}k_{\perp}v_i)$, $v_i^2 = T_i/m_i$, $v_e^2 = T_e/m_e$,

$C_s^2 = T_e/m_i$, $\omega_{\ell h} = \omega_{pi}/(1 + \omega_{pe}^2/\omega_{ce}^2)^{1/2}$, $\omega_k^2 = \omega_{\ell h}^2(1 + m_i k_{||}^2/m_e k^2)$,

ν_e is the electron-ion collision frequency, and γ^* includes any additional sources of energy loss. In particular, because it has been shown that convection of the wave out of the pump resonance cone is the dominant loss mechanism in many realistic heating experiments, we have used a loss rate equal to the transit time of a wave across the resonance cone in some calculations to model the experimental situation.

It is clear from Eqs. (5)- (10) that waves with frequency smaller than the pump frequency are destabilized by the pump and at the same time higher frequency waves are stabilized. If the pump field is strong enough, waves with lower frequency grow until they act as pumps to destabilize still lower frequency waves and stabilize higher frequency waves.

The frequency separation of the decay wave from the pump wave $\Delta\omega$ is proportional to $k\lambda_D\ \omega_{pi}$ and lines of maximum growth rate will be diagonal lines in the (k,ω_k) plane. At short-wavelengths, linear Landau damping will prevent any growth of waves whose wavenumber satisfies $k\lambda_{De} > 1/4\left(1 + \omega_{pe}^2/\omega_{ce}^2\right)^{1/2}$. Thus, the instability will be characterized by a maximum frequency shift of $\Delta\omega_m \simeq 0.25\omega_{\ell h}$. This behavior is shown in Fig. 1 which shows the value of $B(\underset{\sim}{k}'-\underset{\sim}{k},\ \omega_k,-\omega_k)$ maximized as a function of $k_{||}$ when $\underset{\sim}{k}_\perp \cdot \underset{\sim}{k}_\perp' \doteq 0$. It is interesting that short-wavelength pumps can result in frequency shifts as large as $0.1\omega_{\ell h}$. The process

involved in the cascade of energy to lower frequencies is also nonlinear Landau damping and thus, a change in frequency of approximately $\Delta\omega_m$ will occur in each cascade. By integrating over $\underset{\sim}{k}$ and by using the antisymmetric property

$$B(\underset{\sim}{k}'-\underset{\sim}{k},\omega_{\underset{\sim}{k}'},-\omega_{\underset{\sim}{k}}) = -B(\underset{\sim}{k}-\underset{\sim}{k}',\ \omega_{\underset{\sim}{k}}-\omega_{\underset{\sim}{k}'}) \ , \tag{11}$$

we obtain from Eq. (5) the useful and informative conservation law for the plasmon number $I_{\underset{\sim}{k}}$

$$\frac{\partial I}{\partial t} = \int d^3\underset{\sim}{k}\ (\gamma_T + \gamma^{\circ}_{\underset{\sim}{k}}) I_{\underset{\sim}{k}} + S \ , \tag{12}$$

where

$$I = \int d^3\underset{\sim}{k}\ I_{\underset{\sim}{k}} \ .$$

A steady state is reached ($\partial I/\partial t = 0$) with a saturated level of plasmons far exceeding the initial level when the number of plasmons created by the constant amplitude pump equals the number of plasmons lost to the system by Landau damping, collisional damping, or convection. We assume justifiably that S is small and can be neglected at saturation. This law shows that saturation can be achieved only by providing a sink of energy at lower frequencies. In an infinite homogeneous system, the only sinks are creation of high energy tails on the velocity distributions by Landau damping of short wavelength waves and an

increase in electron temperature by collisional damping.

Because in absence of convective losses the decay wave energy will naturally concentrate in collisionally damped modes, strong instabilities, whose growth rate far exceeds the collision frequency, will require many cascades to achieve a saturated state and satisfy the conservation law for plasmon number in steady state

$$\int d^3\underset{\sim}{k}(\gamma_L + \gamma_{\underset{\sim}{k}}^{\circ})\ I_{\underset{\sim}{k}} \simeq 0 \quad , \tag{13}$$

when $\text{Max}|\gamma_{oj}| = \gamma_{om} >> |\gamma_L|$, that is, $\nu_e/\omega_{\ell h} << c^2|E_o^2|/4B_o^2C_s^2\ \omega_{\ell h}/\omega_o$.

In view of the previous discussion, it is clear that only instabilities produced by pumps very near threshold can saturate by cascading. The rate at which plasmons are absorbed is approximately $\nu_e\ I = 2\int d^3\underset{\sim}{k}\gamma_L\ I_{\underset{\sim}{k}}$. The rate at which plasmons are created is $2\gamma_{om}I_1 = P\ \nu_e I_1$ where I_1 is the number of plasmons in linearly unstable modes, and P is the ratio of the pump power to the threshold power. We can estimate the total number of plasmons $I = mI_1$ where m is the number of cascades. Since lower hybrid waves have a minimum frequency $\omega_{\ell h}$, the maximum number of cascades is $M = (\omega_o - \omega_{\ell h})/\Delta\omega_m$. Thus, the conservation law for plasmon number, Eq. (13), puts a limit on P that

$$P < (\omega_o - \omega_{\ell h})/\Delta\omega_m \sim 4(\omega_o - \omega_{\ell h})/\omega_{\ell h} \ . \tag{14}$$

The saturation of decay instabilities including convective losses requires some explanation. The convective loss rate of a wave in the pump resonance cone equals the component of the wave group velocity normal to the pump group velocity in the plane of propaga-

tion of the pump (x-z plane) divided by the width of the resonance cone in this direction. This rate, which depends on the angle the wavenumber makes in the plane normal to the magnetic field, is

$$\gamma^* = \frac{\omega_k^2 - \omega_{\ell h}^2}{\omega_k k_\perp L}\left[\left(\frac{\omega_o^2 - \omega_{\ell h}^2}{\omega_1^2 - \omega_{\ell h}^2}\right)^{1/2} - \cos\psi_{\underset{\sim}{k}}\right]\frac{(m_i/m_e)^{1/2}\omega_{\ell h}}{(\omega_o^2 - \omega_{\ell h}^2)^{1/2}} \quad , \qquad (15)$$

where $\cos\psi_{\underset{\sim}{k}} = k_x/k$ and L is the extent of the antenna in the z direction at the plasma boundary. This rate can only vanish if $k_y = 0$ and $\omega_k = \omega_o$. The combination of the convective loss rate with the Landau damping rate implies a minimum damping rate at a rather short wavelength where the two rates are almost equal. Therefore, the decay wave spectrum will be concentrated at rather short-wavelengths and the cascading process of necessity will involve large frequency shifts. In addition, the threshold for instability will be raised substantially as the minimum damping rate replaces the collision rate in calculating the threshold power.

Implicit in this model is the assumption that the interaction width of secondary decay waves with the primary decay waves excited by the pump is equal to the width of the pump resonance cone. In fact, this is a reasonable assumption because once waves convect out of the resonance cone, i.e., the amplifying medium, they, being such short-wavelength waves, damp rather quickly by linear Landau damping.

An estimate of the steady state plasmon number can be obtained from Eq. (5) by setting the S_k, γ_L, and left hand side equal to zero so that one finds

$$\gamma_{\underset{\sim}{k}}^{NL} + \gamma_{\underset{\sim}{k}}^{o} = 0 \ .$$

Estimating $B(\underset{\sim}{k}'-\underset{\sim}{k}, \omega_{\underset{\sim}{k}} - \omega_{\underset{\sim}{k}})\sin^2(\omega_{\underset{\sim}{k}}-\omega_{\underset{\sim}{k}'})$ by its maximum value in both the linear and nonlinear growth rate, we obtain

$$I = \int d^3\underset{\sim}{k}' \ I_{\underset{\sim}{k}'} = \frac{1}{16\pi} \frac{|E_o|^2}{\omega_o} = I_o \ , \tag{16}$$

or that saturation will occur when the plasmon number of decay waves equals the plasmon number of the pump. An immediate consequence of this dimensional analysis is that the energy in high-frequency decay waves will be smaller than in the pump wave because the frequency shift of the decay wave spectrum is so large. The actual relationship between the decay wave energy and the pump energy can be found from numerical solutions to Eq. (5) which we present in the next section.

III. NUMERICAL SOLUTION OF WAVE KINETIC EQUATION

Direct solution of Eq. (5) requires three-dimensions in wavenumber space. To simplify the calculation, we have assumed that the number density and wave energy are almost isotropic functions of the azimuthal angle ψ_k in wavenumber space. We then average Eq. (5) over the angle ψ_k to obtain an equation for the angle averaged number density I_k. We solve the resulting equation numerically on a wavenumber grid in $(k_\perp, k_{||})$ space. The integral in Eq. (9) is replaced by a sum over discrete modes; the number density is multiplied by the volume element in wavenumber $V_k = 2\pi k_\perp \, dk_\perp dk_{||}$ to obtain the number of plasmons per j^{th} volume element N_j. We then normalized this plasmon number to the plasmon number of the pump $N_o = (1+\omega_{pe}^2/\omega_{ce}^2)|E_o|^2/16\pi\omega_o$. As a result, we obtain a nonlinear time dependent matrix equation for the evolution of the plasmon number N_j,

$$\frac{1}{2}\frac{\partial}{\partial\tau} N_j = (-\gamma_{Lj} + \gamma_{oj} + \sum_i \gamma_{ji}^{NL} N_i) N_j + S_j \, . \qquad (17)$$

Time is normalized with respect to lower hybrid frequency as are the linear and nonlinear growth rates. We introduce the normalized frequency and wavenumber of the j^{th} zone $W_j = \omega(k_j)/\omega_{\ell h}$, $K_j = k_{\perp j}(T_e/m_i\omega_{\ell h}^2)^{1/2}$, and $x_j = k_{||_j}(T_e/m_e\omega_{\ell h}^2)^{1/2}$. Thus the nondimensional growth rates are

$$\gamma_{Lj} = \frac{1}{2}\left(\frac{\pi}{2}\right)^{1/2}\frac{W_j}{K_j^2}\left[\frac{W_j}{K_j}\left(\frac{T_e}{T_i}\right)^{3/2}\exp\left(-\frac{W_j^2 T_e}{2K_j^2 T_i}\right) + \frac{W_j}{x_j}\exp\left(-\frac{W_j^2}{2x_j^2}\right)\right] \tag{18}$$

$$+ \frac{\nu_e}{2\omega_{\ell h}}\left(\frac{\omega_{pe}^2}{\omega_{pe}^2 + \omega_{ce}^2} + \frac{x_j^2}{K_j^2 W_j^2}\right) + \bar{\gamma}^* \quad ,$$

$$\bar{\gamma}^* = \frac{(W_j^2-1)^{1/2}}{W_j}\left(\frac{m_e}{m_i}\right)^{1/2}(K_j\ell)^{-1} \quad , \tag{19}$$

$$\ell = \frac{\omega_{\ell h} L}{C_s} = \frac{L}{\lambda_{De}}\left(1 + \frac{\omega_{pe}^2}{\omega_{ce}^2}\right)^{-1/2} \quad , \tag{20}$$

$$\gamma_{oj} = -\frac{c^2 E_o^2}{16 B_o^2 c_s^2}\frac{W_j}{W_o^2} B(K_j, x_j, W_j - W_o) \quad , \tag{21}$$

$$\gamma_{ji}^{NL} = -\frac{c^2 E_o^2}{16 B_o^2 c_s^2}\frac{1}{W_o} \bar{B}(K_{ij}, x_{ij}, W_{ij}) \quad , \tag{22}$$

where $W_o = \omega_o/\omega_{\ell h}$, $K_{ij}^2 = K_i^2 + K_j^2 - 2K_iK_j \sin^2\psi$,

$x_{ij} = |x_i - x_j|$, $W_{ij} = W_i - W_j$, and

$$\bar{B}(K_{ij},\ x_{ij},\ W_{ij}) = \frac{1}{\pi}\int_{o}^{2\pi} d\psi\ \sin^2\psi\ B(K_{ij},\ x_{ij},\ W_{ij}). \qquad (23)$$

In the numerical solutions to Eq. (17), the thermal corrections to the cold plasma dispersion relation for lower hybrid waves were included with the result that

$$W_j^2 = 1+(x_j^2)/(K_j^2) + 3(x_j^4 + K_j^4)/(x_j^2 + K_j^2) \quad . \qquad (24)$$

The grid size $\Delta(K_j,x_j)$ was chosen to reflect the fact, in the cold plasma approximation, the frequency W_j is constant along curves defined by x/K = const. An adequate representation of $\bar{B}$ is ensured if, on adjacent constant frequency curves, a number of pairs (K_j,x_j) exist such that either

$$(W_j - W_1)/(|K_j^2 + K_1^2|) \quad 1 \quad ,$$

or

$$(W_j - W_i)/(|x_j - x_i|) \sim 1 \ .$$

The representation chosen does satisfy these criteria. The spontaneous emission term becomes $S_j = S_K V_K/N_o\omega_{\ell h}$.

For computational purposes, we set $S_j = K_j \bar{S}$ where $\bar{S}$ is a small constant and the wavenumber dependence of S_j reflects the wavenumber dependence of the volume element V_K. $\bar{S}$ was chosen so that $N_j = \gamma_{Lj} S_j$. The value of $\bar{S}$ has been varied by orders of magnitude without substantially altering the results. This insensitivity is a result of the fact that the saturated intensities of the nonlinearly unstable modes are many orders of magnitude larger than the initial values. The initial value of N_j was determined by setting $N_j = 2K_j N_{jo}/K_{jmax}$ where K_{jmax} is the maximum value of K_j. In all cases reported here, $N_{jo} = 10^{-6}$. Equation (17) was advanced in time with use of a second order explicit integration scheme. The time step was small compared to both the linear and nonlinear growth rates. The (K_j, x_j) wavenumber mesh used was (5,60), (10,30), and (20,15) for a total of 300 zones.

Solutions to Eq. (17) were obtained for $W_o = 1.42$, 2.0, and 4.0 for pump power relative to threshold power between one and six times threshold. Cases were run $\gamma^* = 0$ and $\gamma^* \neq 0$. The results with and without γ^* are similar except that the characteristic frequency shift involved in each cascade is larger and the energy in long-wavelength modes is suppresed when $\gamma^* = 0$.

In Fig. 2 we show an example of the time evolution of the total decay wave energy. There are oscillations of decreasing amplitude in the total energy about the steady state value. An examination of the individual modes shows that this oscillation is a result of an exchange of energy between modes similar to coupled harmonic oscillators. Because these oscillations persist a long time before settling down to a steady state value, we have employed the technique of interrupting the time evolution

after a few oscillations and restarting the system with the instantaneous value of the plasmon number replaced by its time averaged value. This technique saves computational time in finding accurately the total steady state wave energy. The wave energy per volume element is $U_j(K_j, W_j) = 2W_jN_j$. We will present results for U_j, the total energy $U = \sum_j U_j$, and the energy per frequency interval $U(W) = \sum_{j, W_j \in (W, W+\Delta W)} U_j$. Two classes of decay waves are destabilized by the pump. One type is low-phase velocity waves that are convectively amplified to a nonlinear level in one transit across the pump and then damp quickly in space. The other types, high-phase velocity ducted waves, transit around the torus, and thus through the pump many times. These waves are destabilized by the spatially averaged pump electric field. These waves are damped by collisions only and have lower thresholds than the convective modes, but also have correspondingly smaller growth rates. The nonlinear saturation of these waves by cascading is considered in Sec. III. A. The saturation of the convective modes is considered in Sec. III. B.

III.A. Infinite Homogeneous Plasma

In this section, we set $\gamma^* = 0$ and present the results of numerical solutions to Eq. (17) for pump frequencies in the range 1-4 times the lower hybrid frequency and pump powers 1-6 times the threshold power. The threshold power is determined by the collision frequency, which is very small compared to both the lower hybrid frequency and the acoustic frequency. Thus, the nonlinear time evolution scales with the collision frequency.

In Fig. 2, we show that time history of the total decay wave energy normalized to the pump energy for $\omega_o = 1.42\omega_{\ell h}$ and $P = 1.3$. The characteristic oscillation in energy discussed in the previous section is apparent. For pump frequencies in this range, only one cascade is available to the linear unstable modes before the minimum frequency mode is destabilized. Therefore, saturation by cascading will not be an effective saturating mechanism for the decay instability in this frequency range as is evident in Figs. 3, 4, and 5.

In Fig. 3, we show the frequency spectra when $\omega_o = 1.42\omega_{\ell h}$ and for pumps 1.3 and 3.0 times threshold. In the former case, the energy in lower frequency modes is smaller than the energy in pumped modes and is below the energy necessary to destabilize the nonexistent lower frequency modes. However, the energy in the lowest frequency mode in the latter case is above threshold for destabilizing other modes. Since no further cascading is possible, the energy in these modes will continue to increase until the threshold for other nonlinear processes to occur is surpassed. We will return to this question of condensation in the concluding section. Figure 4 shows the two-dimensional energy spectra for $P = 1.3$, which shows that the energy is concentrated in collisionally damped waves. There is significant energy in the longest wavelength lowest frequency mode, but its energy is still much smaller than the pump energy and is below threshold. Figure 5 shows the two-dimensional spectra for $P = 2.0$. There is a dramatic increase in the energy in the lowest frequency longest wavelength mode to the level where it

would be above threshold for destabilizing lower frequency modes if they existed.

The condensation phenomenon outlined above differs from the collapse phenomena separated by Musker and Sturman[9] in the following way. Our calculations have a constant driving force and show that wave energy accumulates secularly in regions of long-wavelength and perpendicular propagation ($k_{||}^2/k^2 << m_e/m_i$). The Musker and Sturman calculation concentrates on the region where the thermal corrections to the dispersion relation [see (24)] dominate the angular cold plasma terms. The problem, then, becomes two-dimensional, and they demonstrate by a numerical calculation that a collapse phenomena occurs for a fixed amount of wave energy. Since our computations show that the wave energy accumulates in the long-wavelength reguire where the thermal corrections are very small, the adequacy of the two-dimensional model remains in question.

For $\omega_o = 4.05\omega_{\ell h}$, the available wavenumber space for cascading is much larger and cascading is an effective means for saturation of the decay instability up to powers 8-10 times threshold. The solution to Eq. (17) was studied for pump powers in the range 1-6 times threshold. The frequency spectra obtained for P = 2. and 4. are shown in Fig. 6. These spectra are similar to the Langmuir-ion acoustic decay instability where a series of peaks separated by acoustic frequencies is observed.

III.B. Cascading with Convective Loss

In this section a finite value of γ^* is used which inhibits the growth of long wavelength modes due to the short transit time such modes have. The total linear dissipation rate then has a minimum as a function of wavenumber. For the parameters chosen, collisional damping is negligible and the most unstable waves are ordinarily strongly Landau damped. As a result, the threshold is much higher, the frequency shifts are larger since only rather short-wavelength modes can interact, and the nonlinear growth time scales with the convective loss rate and linear Landau damping rate. The various time scales obey the inequalities

$$\omega_{\ell h}^{-1} < \omega_A^{-1} << \gamma^{*-1} > \simeq \gamma_L^{-1} \simeq \gamma^{NL-1} .$$

Examination of Eq. (20) shows that $<\gamma^*> \to 0$ as $W_j \to 1$ so that convection will not be effective in preventing condensation. Moreover the concept of group velocity is not valid in the vicinity of turning points or resonances which are implied by the frequency approaching the lower hybrid frequency as can be seen directly from the dispersion relation (24). We limit ourselves therefore to the consequences of including convective loss in the wave kinetic equation when $\omega_o = 4\omega_{\ell h}$. The two dimensional energy spectra for P = 4 with convective loss is shown in Fig. 7. The energy has spread to waves that are strongly Landau damped. The coupling of short-wavelength waves to long wavelengths where the coupling is strongest (see Fig. 1) is inhibited by the inclusion of convective loss. Most of the energy is concentrated in waves with $K \simeq 0.2$. In Fig. 8 we show a comparison of the frequency spectra for P = 4 with and without

convective losses. Two features are apparent. First, the initial frequency shift of the spectrum away from the pump is larger with convection. The second feature is the spread of the spectrum closer to the point $\omega_k = \omega_{\ell h}$ with convective damping for the same power relative to threshold. This is a result of the suppression of long wavelengths by convective loss and the larger absolute value of the pump power which parametrically destabilizes shorter wavelength more highly damped modes. We expect that the relative power required to destabilize the minimum frequency mode will be lower in this case. This expectation is confirmed by the frequency spectrum for P = 6 in Fig. 9, which shows that the decay wave spectrum has spread to $\omega_k \sim \omega_{\ell h}$. One of the main results of this paper is that strong pumps do not saturate by cascading. Either a strong turbulence theory or other nonlinear or nonuniformity effects will be required to follow strong pump instabilities to a nonlinear steady state.

Another characteristic of the spectra with convective loss is that they are continuous as a function of frequency unlike the discrete spectra without convective loss. These convective damping spectra are similar to the spectra observed by Porkolab, et al, during radio-frequency heating experiments on Adiabatic Toroidal Compressor.[4]

The saturation by cascading of the parametric decay instability for electron plasma waves has been treated by Rubenchik, et al., for the case that $\omega_{ce} >> \omega_{pe}$ and $\omega_{pe} \gtrsim \omega_o >> \omega_{\ell h}$. In this case, the ion motion can be neglected so the frequency dispersion becomes $\omega = \omega_{pe} k_{||}/k$. Outstanding differences in treatment were that the nonlinear coupling arises from motion along the field lines rather than $\underset{\sim}{E} \times \underset{\sim}{B}$ drift across the field lines, and the scattering was only due to ions rather than the roughly equal contributions from ions and electrons for the cases treated in this paper. By far, the

largest discrepancy in results was that Rubenchik, et.al., obtain a saturated spectrum that was concentrated in short-wavelength modes rather than long wavelengths in the corresponding cases, i.e. no convective damping. We believe that this result is an artifact of the use in Rubenchik, et.al., of a differential form for the nonlinear scattering term as was done in early treatments of the saturation of the Langmuir decay instability.[12] In the Langmuir case, this approximation led to a spectrum sharply peaked in the angle $\theta = \cos^{-1}(\hat{\underset{\sim}{k}} \cdot \hat{\underset{\sim}{E}}_o)$ where $\hat{\underset{\sim}{k}} = \underset{\sim}{k}/|k|$ and $\hat{\underset{\sim}{E}}_o = \underset{\sim}{E}_o/|\underset{\sim}{E}_o|$, whereas numerical solutions[13] showed that the spectrum was much broader in angle. In the lower hybrid case, the $k_{||}/k$ replaces $k\lambda_{De}$ and $k\lambda_{De}$ replaces θ. Thus, one might expect to obtain a spectrum continuous in $k_{||}/k$ and peaked in $k\lambda_{De}$ from the differential form.

IV. PUMP DEPLETION AND HEATING

The experimental evidence and theoretical analysis have shown that current heating experiments are operating in a range of pump powers that is adequately described by weak turbulence theory - especially when one includes convective loss.

It is important in future experiments to avoid serious pump depletion in the low-density plasma near the surface in order to deliver the pump energy to the main plasma. It is valuable therefore to know the anomalous damping rate of the pump γ_{eff}, that is, the rate of energy loss by the pump due to nonlinear effects. From the conservation law for plasmons, we have

$$\frac{\gamma_{eff}}{\omega_o} \mathcal{E}_o = \gamma_{eff} I_o = 2 \int d^3\underset{\sim}{k}\, \gamma_{\underset{\sim}{k}} I_{\underset{\sim}{k}} .$$

If $\gamma^* = 0$, then $\gamma_k \simeq \nu_e/2$ and

$$\gamma_{eff} \mathcal{E}_o = \omega_o \nu_e \int d^3\underset{\sim}{k}\, I_{\underset{\sim}{k}} = \nu_{ei} \int d^3\underset{\sim}{k}\, I_{\underset{\sim}{k}} . \tag{25}$$

The total number of plasmons $I = \int d^3\underset{\sim}{k}\, I_{\underset{\sim}{k}}$ as a function of pump power has been found from the numerical results to obey the approximate solution

$$I = 0.5p\, I_o , \tag{26}$$

and thus

$$\gamma_{eff} = 0.5\nu_e P \ . \tag{27}$$

When convective losses are included, the damping rate is wave-number dependent. In Fig. 10, we present the results of a numberical evolution of the total decay wave plasmon number versus pump power. By comparing the dependence of the effective damping rate for the pump on P where

$$\gamma_{eff} = 2 \int d^3\underset{\sim}{k}\ \gamma_k\ (I_k/I_o) \tag{28}$$

and the dependence of the total decay wave plasmon number on P, we find that, to a good approximation,

$$\gamma_{eff} = 2\alpha\bar{\gamma}P \ , \tag{29}$$

where α is a coefficient of order unity; $\bar{\gamma}$ is the minimum damping rate and has the approximate value

$$\bar{\gamma} = v_{gk}/L \ , \tag{30}$$

where L denotes the length of the waveguide array along the magnetic field. Using Eq. (29) and the radial group velocity for the pump,

$$v_{gxo} = -\frac{(\omega_o^2 - \omega_{\ell h}^2)}{\omega_o}\ \frac{k_{xo}}{k_{\perp_o}^2} = -\frac{(\omega_o^2 - \omega_{\ell h}^2)^{3/2}}{\omega_o\ \omega_{\ell h}\ k_{o\|}} \left(\frac{m_e}{m_i}\right)^{1/2} \tag{31}$$

we obtain an equation governing the depletion of the pump power Π

$$\frac{\partial \Pi}{\partial r} = -\frac{1}{L_{abs}} \left(\frac{\Pi^2}{\Pi_{th}}\right) \tag{32}$$

where the absorption length L_{abs} is given by

$$L_{abs} = \frac{\omega_o}{\omega_{pe}} \frac{(k\lambda_{De})}{N_{||}} \left(\frac{m_e c^2}{T_e}\right)^{1/2} \left(\frac{L}{\alpha}\right) \tag{33}$$

where $N_{||} = ck_{||o}/\omega_o$. The absorption length in Eq. (33) is valid only when $\omega_o >> \omega_{\ell h}$, which is the primary region of interest here. From Eq. (7) of Ref. 3, we have at radius r the threshold formula,

$$\Pi_{TH} = \frac{9(2\pi)^{1/2}}{k\lambda_{De} N_{||}} \frac{r}{a} \frac{B^2}{\omega_{pi}^2} \left(\frac{T_e}{m_1}\right)^{3/2} \tag{34}$$

where a is the minor radius. This formula is appropriate if $T_e >> T_i$ and $\omega_o >> \omega_{\ell h}$. However, the scaling of the threshold with density and temperature is independent of these assumptions. Let us assume that both the electron temperature and the density have a parabolic profile so that in terms of the central temperature and central density,

$$n(r)/n(0) = T_e(r)/T_e(0) = (1 - r^2/a^2) \ . \tag{35}$$

Using Eqs. (32)-(35), we obtain

$$\frac{d\Pi}{dr} = - \frac{N_{||}^2}{9(2\pi)^{1/2}} \left(\frac{m_i}{m_e}\right)^{1/2} \frac{\alpha}{B^2 cL} \frac{a}{r} \frac{\omega_{pe}}{\omega_o} \frac{1}{\lambda_{De}^2} \Pi^2 \ , \tag{36}$$

$$= - [1 - (r^2/a^2)]^{1/2} \Pi^2/r\Pi_N$$

provided $\Pi \geq \Pi_{TH}$. We defined

$$\Pi_N = \frac{9(2\pi)^{1/2}}{\alpha N_{||}^2}\left(\frac{\omega_o}{\omega_{pi}}\right)\frac{B^2C}{\omega_{pe}^2}\ \frac{L}{a}\left(\frac{T_e}{m_i}\right) \tag{37}$$

$$= (7\ \text{Megawatts})\left(\frac{T_e}{\text{keV}}\right)\left(\frac{10^{13}\text{cm}^{-3}}{n_e}\right)\left(\frac{1}{N_{||}^2}\right)\left(\frac{B}{50\text{kG}}\right)^2\left(\frac{L}{a}\right)\left(\frac{f_o}{1\text{GH}_z}\right)\left(\frac{0.8}{\alpha}\right)$$

in terms of the central values of the electron temperature and density and neglected the weak radial dependence of the magnetic field. Let us define r_o as the radius at which $\Pi = \Pi_{TH}$. The pump power at radius $r > r_o$ is then

$$\Pi = [\Pi_o]/[1 + \Pi_o f(r/a)/\Pi_N] \tag{38}$$

where Π_o is the incident power and

$$f(r/a) = \int_{r/a}^{'} dx/x\ (1 - x^2)^{1/2}$$
$$= -\ (1 - r^2/a^2)^{1/2} + \ell n\left\{\text{tg}[\pi/4 + 1/2\ \cos^{-1}(r/a)]\right\}. \tag{39}$$

The functional dependence on radius given in Eq. (39) is, of course, sensitive to the radial profile one assumes for the temperature and density dependence. Figure 11 presents a graph of $f(r/a)$ and $1/f(r/a)$. Formula (38) also shows that there is a limiting power Π_{max} given by

$$\Pi_{max} = \Pi_N/f(r/a) \tag{40}$$

which governs the maximum power which can penetrate past a given radius r. More important is the scaling implied in Eq. (37) which shows that pump penetration improves for small

parallel index of refraction, large magnetic field, high temperature, and small densities. The most unfavorable scaling is the inverse linear dependence of Π_N on the plasma radius a.

Equations (34) and (35) make it clear that the threshold is a decreasing function of radius r due to the strong dependence on temperature. Equations (33)-(37) are valid only when $\omega_o >> \omega_{\ell h}$. In fact, the threshold for the convective quasi-mode is also low in the plasma interior if $\omega_o \leq 1.5\omega_{\ell h}$, because the decay waves then have small group velocities as can be seen from Eq. (31), and because the pump electric fields are strongest there provided no severe pump depletion has taken place at the plasma surface. If the incident power is less than the maximum value of the threshold power, then a radius r_o, for which the power equals the threshold power, will exist in the plasma periphery. We have calculated the percentage of the incident power that is absorbed by the plasma surface between $r = r_o$ and $r = a$. This fraction of the power is wasted heating the surface plasma (the plasma between $r = r_o$ and $r = a$) and is unavailable to heat the main plasma. Evaluating Eq. (37) for Adiabatic Toroidal Compressor, we assume $n = 3 \times 10^{13} cm^{-3}$, $\omega_o = 5 \times 10^9 sec^{-1}$, $T_e = 800$ eV, $B = 17$kG, $a = 17$ cm, $L = 20$ cm, $N_{||} = 2.7$ and $\alpha = 0.5$. For a typical incident power $\Pi_o = 100$ KW, $r_o/a = 0.98$, only 2% of the power is absorbed by the surface plasma and pump depletion is not a problem. However if $N_{||} = 5.5$, which provides better accessibility and is typical of some of the waveguide launchers used on Adiabatic Toroidal Compressor, then 15% of the power is absorbed by the surface plasma. In Fig. 12 we show, based on

Eq. (39), the fraction of incident power absorbed by the surface plasma as a function of incident power for Adiabatic Toroidal Compressor and Poloidal Divertor Experiment parameters for $N_{||} = 2.7$ and 5.5. For Poloidal Divertor Experiment, we assume $n = 3 \times 10^{13} cm^{-3}$, $\omega_o = 5 \times 10^9$, $T_e = 1.3$ keV, $B_o = 25$kG, $a = 45$ cm, $L = 24$ cm. The importance of tailoring the wavenumber dependence of the pump spectrum so that the parallel index of refraction is small i.e., $N_{||} \lesssim 2$ but yet satisfies the accessibility criterion $N_{||} \lesssim 1.4$ is clear from a comparison of the surface absorption for the same power Π_o but different values of $N_{||}$. The parallel index of refraction $N_{||}$ is important for two reasons. First, larger values of $N_{||}$ for the same incident power lower the threshold for instabilities by increasing the pump electric field. Second, the slower group velocity decreases the scale length for pump depletion for a given anomalous damping rate. The threshold formula (33) is modified when $T_e \lesssim 3T_i$ because the parametric decay instability is weaker when the low-frequency mode is nonresonant. In fact, the threshold is about ten times higher if $T_e = T_i$ than Eq. (33) indicates. However, the exact value of the electron to ion-temperature ratio is unknown in tokamaks and is undoubtedly a function of the minor radius because the impurities and neutrals at the plasma edge probably cool the ions and keep $T_e >> T_i$ although the temperature ratio is closer to one inside because of the good perpendicular ion-thermal conductivity and poor electron perpendicular conductivity. However, if the divertor on Poloidal Divertor Experiment is effective in controlling impurities, one might expect the threshold

formula (33) to be an underestimate. If the threshold is doubled at all radii, then the same percentage of power is absorbed by the edge plasma if the incident power is doubled.

The plasma heating rate can be found from knowledge of the steady state energy spectrum of lower hybrid waves. The anomalous damping rate for the pump gives the rate at which pump wave energy ε_o is converted to particle energy ε_p, i.e.:

$$(\partial\varepsilon_p)/(\partial t) = \gamma_{eff}\varepsilon_o \ .$$

More interesting is to predict how the energy will be deposited in the plasma. First, one must establish the percentage of energy in the beat wave ε_B, which is converted directly to thermal velocity electrons streaming along the field lines and thermal velocity ions traveling across the field lines. From conservation of energy in steady state, one finds $\varepsilon_B \simeq \Delta\omega I$ where $\Delta\omega$ is the characteristic frequency shift in each cascade. Because of the large shift in frequency of the steady state spectrum from the pump waves, this energy flow to particles is significant, i.e. $\varepsilon_B \approx \frac{\Delta\omega}{\omega}\ \varepsilon_p \sim 0.25\varepsilon_p$. The details of the division of energy between electrons and ions from the beat wave depends on the beat wave energy density which do not solve for here. For an infinite homogeneous plasma, the high-frequency decay wave spectrum is concentrated in long-wavelength collisionally damped modes, and thus the main body electrons are heated. When convection is important, the decay wave energy is concentrated in short-wavelength waves such that $k\lambda_{De} \sim 0.25$. If $\omega_k >> \omega_{\ell h}$, the energy is deposited in somewhat superthermal

electrons with $v_{||} \sim 4v_e$ but if $\omega_k \lesssim \sqrt{2}\ \omega_{\ell h}$, the energy is deposited in superthermal ions with $v_\perp \sim 4v_i$. Clearly most of the pump energy creates a tail on the electron distribution. Any superthermal ions are the result of beat wave heating and represent a fraction of the total heating.

Let us now turn to the nonlinear absorption produced by high-phase velocity lower hybrid waves, which are ducted around the torus by density profile and destabilized by the spatially averaged electric field. In the linear regime, these waves are damped by electron-ion collisions. The appropriate model for ducted waves is the infinite homogeneous plasma model of Sec. III.A. (i.e. no convective losses) with a pump field given by the spatially averaged electric field. Reference 3 has shown that ducted waves can be above threshold in many tokamaks. Our nonlinear calculations show that for the infinite homogeneous plasma model, only high-phase velocity waves reach important nonlinear intensities (see Fig. 6). Since the effective collision frequency for these waves will be of the order of the electron-ion collision frequency they serve to augment the collisional damping. But since collisional damping is too weak to play an important role in tokamak heating, the high-phase velocity waves do not contribute significantly to plasma heating.

V. CONCLUSIONS AND APPLICATIONS

Radio-frequency heating near the lower hybrid frequency is an attractive means for heating tokamaks because the power can be delivered to the plasma without the need for structures inside the vacuum vessel wall as other lower frequency wave heating mechanisms require. The most serious obstacles to successful tokamak heating are that 1) the threshold for nonlinear processes may be so low in the low-density plasma near the limiter that the pump power is dissipated there rather than in heating the central plasma; 2) the wave energy appears to be transferred primarily to electrons located in the tail of the distribution and streaming along the toroidal field lines; 3) waveguides must be designed so that the Fourier decomposition of the power spectrum has a very well defined parallel wavelength. The question of thresholds is addressed in a companion paper. We show in Sec. III that the power incident from each waveguide array must be kept within a few times threshold near the plasma surface to avoid severe pump depletion. Moreover, this requirement becomes more stringent as the minor radius increases and as the parallel wavelength becomes shorter. The fact that the threshold increases with toroidal magnetic field and with the plasma temperature is favorable to larger tokamaks. The second obstacle has two implications. First, experimental evidence that the tail electrons are actually accelerated was difficult to obtain in Adiabatic Toroidal Compressor since the bremsstrahlung radiation from $8T_e$ electrons did not lie within the range of the detectors. Second, there is evidence from

neutral beam injection experiments that electron temperature increases are difficult to obtain in present-day tokamaks. If this confinement problem continues with larger devices, the tokamak fusion program in general and lower hybrid heating in particular, face a difficult future. The third obstacle is less fundamental. We have shown that it is highly advantageous for the purpose of avoiding pump depletion that high parallel index of refraction components ($N_{||} > 2$) not be imposed by the waveguide launcher. The small components ($N_{||} \lesssim 1.4$) that do not satisfy the accessiblity criteria will not penetrate to the plasma interior but will be confined to the low-density region. Practical considerations demand that we put as much power as possible through one waveguide launcher to minimize the number of launchers required for significant heating. Thus, in order not to waste a large fraction of power heating the plasma periphery, the waveguide array should be designed to launch only waves with parallel index of refraction between 1.4 and 2.0.

If the pump wave energy does penetrate to the plasma interior, the threshold for decay is certainly exceeded. We have shown, however, that a steady state will not be produced within the context of the cascading model even for relatively modest pump powers. A model adequate to predict saturation, the resultant heating rate, and the details of the energy deposition will need to include such nonlinear processes as the oscillating two stream instability, the coupling of three lower hybrid waves,[14] nonlinear frequency shifts, and phase correlation effects,[9] as well as nonuniform plasma effects. However if $\omega_o \gg \omega_{\ell h}$, we have

shown that steady state solutions to the wave kinetic equations do exist for pump powers many times threshold. Many experiments[15] have demonstrated for $\omega_o \sim 1\text{-}10\omega_{\ell h}$ the occurrence of parametric instabilities. However, direct comparison is difficult because the physical parameters are very different from the ones assumed in this paper. Also as we have shown, this case is important in estimating the amount of pump depletion that occurs in the low-density edge region of a tokamak plasma.

ACKNOWLEDGEMENTS

We wish to thank W. Hooke, M. Porkolab, R. Motley, and C. Oberman for their assistance and discussions on this paper.

This work was supported by U. S. Energy Research and Development Administration Contract E(11-1)-3073.

APPENDIX

We follow the treatment in Ref. 16 but restrict our attention to electrostatic waves. We assume a large amplitude wave

$$\underset{\sim}{E}_o(x,t) = E_o \cos(\underset{\sim}{k}_o \cdot \underset{\sim}{x} - \omega_o t)$$

$$= \frac{1}{2} E_{o+} \exp(i\underset{\sim}{k}_o \cdot \underset{\sim}{x} - i\omega_o t) + \frac{1}{2} E_{o-} \exp(-i\underset{\sim}{k}_o \cdot \underset{\sim}{x} + i\omega_o t)$$

which couples the low-frequency electron density fluctuations $\delta n_e(\underset{\sim}{k},\omega)$ to high-frequency lower hybrid sidebands at $\omega_\pm = \omega \pm \omega_o$ $\underset{\sim}{k}_\pm = \underset{\sim}{k} \pm \underset{\sim}{k}_o$. The Fourier transform of Poisson's equation leads to the equation

$$\omega_\pm^2 \varepsilon(\underset{\sim}{k}_\pm, \omega_\pm)\phi_\pm = \left(4\pi ec \,/\, 2k_\pm^2 B_o\right)\omega_\pm \underset{\sim}{k}_\pm \cdot (\hat{\underset{\sim}{e}}_z \times \underset{\sim}{E}_{o+})\delta n_e(\underset{\sim}{k},\omega) \qquad \text{(A1)}$$

where $\varepsilon(\underset{\sim}{k}_\pm, \omega_\pm)$ is the high-frequency lower hybrid dispersion relation for the sidebands. In the low-frequency equations, we keep the bare fluctuating ion microdensity

$$S_{ji}(\underset{\sim}{k},\omega) = (2\pi)^{-3} \sum_i \exp(-i\underset{\sim}{k} \cdot \underset{\sim}{x}_{oj})\delta(\omega - \underset{\sim}{k} \cdot \underset{\sim}{v}_j) \qquad \text{(A2)}$$

and electron microdensity

$$S_e(\underset{\sim}{k},\omega) = (2\pi)^{-3} \sum_e \exp(-i\underset{\sim}{k} \cdot \underset{\sim}{x}_{oe})\delta(\omega - k_\parallel v_{\parallel e}) J_o(k_\perp v_\perp \,/\, \omega_{ce}) \qquad \text{(A3)}$$

where J_o is the Bessel function, and we assume unmagnetized ions and strongly

magnetized electrons. We, thus, arrive at the equations

$$\delta n_e(\underset{\sim}{k},\omega) = (k^2 \ / \ 4\pi e)\chi_e(\underset{\sim}{k},\omega)[\phi(\underset{\sim}{k},\omega) + \psi(\underset{\sim}{k},\omega)] + S_e(\underset{\sim}{k},\omega) \quad , \tag{A4}$$

$$\delta n_i(\underset{\sim}{k},\omega) = (-k^2 \ / \ 4\pi e)\chi_i(\underset{\sim}{k},\omega)\phi(\underset{\sim}{k},\omega) + S_i(\underset{\sim}{k},\omega) \quad , \tag{A5}$$

and

$$k^2\phi(\underset{\sim}{k},\omega) = 4\pi e \ (\delta n_i - \delta n_e) \quad . \tag{A6}$$

The ψ's are the linear susceptabilities and $\psi(k,\omega)$ is the pondermotive potential

$$\psi(\underset{\sim}{k},\omega) = \frac{-ce_{\sim z}}{2B_o} \cdot \left((\underset{\sim}{k} \times \underset{\sim o-}{E}) \phi_+ \ \frac{k_{||+}}{\omega_+ k_{||}} \ + \ (\underset{\sim}{k} \times \underset{\sim o+}{E}) \phi_- \ \frac{k_{||-}}{k_{||}\omega_-} \right) . \tag{A7}$$

Solving Eqs. (A4)-(A6) for $\delta n_e(k,\omega)$, we obtain

$$\delta n_e = [\varepsilon(\underset{\sim}{k},\omega)]^{-1}\left(\chi_e(\underset{\sim}{k},\omega) S_i + [1 + \chi_i(\underset{\sim}{k},\omega)] S_e \ - (k^2\psi/4\pi e)\chi_e(1 + \chi_i) \right) \tag{A8}$$

where $\varepsilon = 1 + \chi_e + \chi_i$ is the low-frequency dispersion relation. Equation (A8) is substituted in Eq. (A1) to obtain

$$\psi^{\pm} = - (\omega_{\pm}^2 \varepsilon^{nl})^{-1} \ \frac{4\pi e}{\varepsilon(\underset{\sim}{k}_{\pm},\omega_{\pm})} \ \frac{c}{2B_o} \ \frac{\omega_{\pm}}{k_{\pm}^2} \ \hat{\underset{\sim}{e}}_z \cdot (\underset{\sim}{k} \times \underset{\sim o\pm}{E}) \tag{A9}$$

$$\cdot \left(\chi_e(\underset{\sim}{k},\omega) S_i + [1 + \chi_i(\underset{\sim}{k},\omega) S_e] \right),$$

where

$$\varepsilon^{nl} = \varepsilon(\underset{\sim}{k},\omega) - k^2 \frac{c^2 |\underset{\sim}{k}\times \underset{\sim}{E}_o|^2}{4B_o^2 k_{||}} \chi_e(k,\omega)[1+\chi_i(\underset{\sim}{k},\omega)]$$

$$\cdot \left(\frac{k_{||+}}{k_+^2 \omega_+^2} \frac{1}{\varepsilon(\underset{\sim}{k}_+,\omega_+)} + \frac{k_{||-}}{k_-^2\omega_-^2} \frac{1}{\varepsilon(\underset{\sim}{k}_-,\omega_-)} \right) \cdot$$

Using the results[16]

$$\langle S_{i_1}(\underset{\sim}{k},\omega) S^*_{i_2}(\underset{\sim}{k}',\omega')\rangle = \frac{n_o}{(2\pi)^3} \delta(\underset{\sim}{k}-\underset{\sim}{k}')\delta(\omega-\omega')\delta_{i_1,i_2} \int d^3v\, f_{i_1}(\underset{\sim}{v})\delta(\omega - \underset{\sim}{k}\cdot\underset{\sim}{v}) , \tag{A11}$$

and

$$\langle S_{e_1}(\underset{\sim}{k},\omega) S^*_{e_2}(\underset{\sim}{k}',\omega')\rangle = \frac{n_o}{(2\pi)^3} \delta(\underset{\sim}{k}-\underset{\sim}{k}')\delta(\omega-\omega')\delta_{e_1,e_2}$$

$$\cdot \int d^3v\, f_{e_1}(\underset{\sim}{v})\delta(\omega - k_{||}v_{||}) J_o^2(k_\perp v_\perp/\omega_{ce}) , \tag{A12}$$

we can compute the ensemble average electric field energy density

$$\langle |E(x,t)|^2\rangle = \int d^3k \langle |E_k|^2\rangle = \frac{1}{4} \frac{n_o}{(2\pi)^3} \left(\frac{\omega_{pe}^2}{n_o}\right)^2 \frac{1}{\omega_{ce}^2} \int d^3k \int d\omega$$

$$[|\chi_e(\underset{\sim}{k},\omega)|^2 \tilde{f}_i(\omega/k) + |1+\chi_i(\underset{\sim}{k},\omega)|^2 \tilde{f}_e(\omega/k_{||})]$$

$$\left(\frac{|\underset{\sim}{k}_+ \times \underset{\sim}{E}_{o_+}|^2}{\omega_+^2 |\varepsilon_+|^2 k_+^2} + \frac{|\underset{\sim}{k}_- \times \underset{\sim}{E}_{o_-}|^2}{\omega_-^2 k_-^2 |\varepsilon_-|^2} \right) , \tag{A13}$$

where

$$\tilde{f}_i(\omega/k) = \int d^3v\ f_i(\underset{\sim}{v})\,\delta(\omega - \underset{\sim}{k}\cdot\underset{\sim}{v}) \quad , \tag{A14}$$

and

$$\tilde{f}_e(\omega/k_{||}) = \int d^3v\ f_e(\underset{\sim}{v})\,\delta(\omega - k_{||}v_{||})\,J_o^2(k_\perp v_\perp/\omega_{ce}) \quad . \tag{A15}$$

Here $\langle\ \rangle$ denotes the ensemble average.

Of particular interest, here, is the case of nonresonant decay of the pump wave to a lower hybrid wave by scattering off the ions and electrons. In this case, $\varepsilon_- \approx 0$ and $\varepsilon_+ \neq 0$ so that

$$\varepsilon_- = -\frac{2(1+\omega_{pe}^2/\omega_{ce}^2)}{\omega_e(\underset{\sim}{k}-\underset{\sim}{k}_o)}\left[\omega_- + \omega_e(\underset{\sim}{k}-\underset{\sim}{k}_o) + i\gamma_L(\underset{\sim}{k}-\underset{\sim}{k}_o)\right] ,$$

and ω_e and γ_L are the linear frequency dispersion relation and damping rate respectively for lower hybrid waves and

$$\begin{aligned}\varepsilon^{nl}\varepsilon_- &= -\frac{2(1+\omega_{pe}^2/\omega_{ce}^2)}{\omega_e(\underset{\sim}{k}-\underset{\sim}{k}_o)}\ \varepsilon(\underset{\sim}{k},\omega)\left[\omega_- + \omega_e(\underset{\sim}{k}-\underset{\sim}{k}_o) + i\gamma_e(\underset{\sim}{k}-\underset{\sim}{k}_o)\right] \\ &\quad - \frac{k^2}{k_-^2}\ \frac{c^2|\underset{\sim}{k}\times\underset{\sim}{E}_o|^2}{4B_o^2}\ \frac{k_{||}-\chi_e(\underset{\sim}{k},\omega)}{k_{||}\omega_e^2(\underset{\sim}{k}-\underset{\sim}{k}_o)}\left[1+\chi_i(\underset{\sim}{k},\omega)\right] \\ &\approx -\frac{2(1+\omega_{pe}^2/\omega_{ce}^2)}{\omega_e(\underset{\sim}{k}-\underset{\sim}{k}_o)}\ \varepsilon(\underset{\sim}{k},\omega)\left[\omega_- + \omega_e(\underset{\sim}{k}-\underset{\sim}{k}_o) + i\gamma_{nl}\right] \quad ,\end{aligned} \tag{A16}$$

where

$$\gamma_{nl} \approx \gamma_e(\underset{\sim}{k}-\underset{\sim}{k}_o) + \frac{c^2|\underset{\sim}{k}\times\underset{\sim}{E}_o|^2}{8B_o^2(1+\omega_{pe}^2/\omega_{ce}^2)}\ \frac{k^2 k_{||}-}{k_{||}\omega_e(\underset{\sim}{k}-\underset{\sim}{k}_o)k_-^2}\ \mathrm{Im}\left(\frac{\chi_e(\underset{\sim}{k},\omega)\left[1+\chi_i(\underset{\sim}{k},\omega)\right]}{\varepsilon(\underset{\sim}{k},\omega)}\right) . \tag{A17}$$

Substituting Eq. (A17) into Eq. (A13), integrating over ω and picking up the contribution from the resonance at $\omega_- = -\omega_e(\underset{\sim}{k} - \underset{\sim}{k}_o)$, we obtain the result for Maxwellian velocity distributions

$$I_k = \frac{(1 + \omega_{pe}^2/\omega_{ce}^2)}{4\pi\omega_k} \frac{\langle|E_k|^2\rangle}{(2\pi)^3}$$

$$= (2\pi)^{-6}\left(\frac{\pi}{2}\right)^{\frac{1}{2}}\gamma_{nl}^{-1} \frac{\omega_{\ell h}}{\omega_k} \frac{T_e}{16} \frac{c^2|\underset{\sim}{k} \times \underset{\sim}{E}_o|^2}{B_o^2 C_s^2 k^2} G(\underset{\sim}{k}, \omega_k - \omega_o) \quad . \qquad \text{(A18)}$$

The spontaneous emission follows from (A18) by identifying $S_k = \gamma_{nl} I_k$. The generalization to a spectrum of waves follows by assuming all waves are incoherent.

REFERENCES

[1]W.M. Hooke, Bull. Am. Phys. Soc. 20, 1313 (1975); V.V. Alikaev, Yu. I. Arsen'ev, G.A. Bobrovskii, V.I. Poznyak, K.A. Razumona, and Yu. A. Sokolov, Zh. Tekh. Fiz. 45, 523 (1975), [Sov. Phys. Tech. Phys. 20, 327 (1975)].

[2]M. Brambilla, Nucl. Fusion 16, 47 (1976).

[3]R.L. Berger, Liu Chen, P.K. Kaw, and F.W. Perkins, "Lower Hybrid Parametric Instabilities - Nonuniform Pump Waves and Tokamak Applications," (to be published in Phys. Fluids).

[4]M. Porkolab, Bull. Am. Phys. Soc. 20, 1313 (1975).

[5]P.A. Boyd, F.J. Stauffer, and A.W. Trivelpiece, Phys. Rev. Letters 37, 98 (1976).

[6]G.J. Morales and Y.C. Lee, Phys. Rev. Letters 35, 930 (1975).

[7]P.K. Kaw, "Filamentation Instability of Lower Hybrid Waves in a Plasma," Princeton Report - MATT - 1208.

[8]J. Dawson and C. Oberman, Phys. Fluids 2, 103 (1959); R.K. Fisher and P.W. Gould, Phys. Fluids 14, 857 (1971); R.J. Riggs and P.R. Parker, Phys. Rev. Letters 29, 852 (1972); P. Bellan and M. Porkolab, Phys. Fluids 17, 1592 (1974).

[9]S.L. Musker and B.I. Sturman, Pis'ma Zh. Eksp. Teor. Fiz 22, 537 (1975) [JETP Lett. 22, 265 (1975)].

[10]A. Hasegawa and Liu Chen, Phys. Fluids 18, 1321 (1975); A. Rogister, Phys. Rev. Letters, 34, 80 (1975); A.M. Rubenchik, Yu. Rybak, and B.I. Sturman, Zh. Eksp. Teor. Fiz 67, 1364 (1975) [Sov. Phys. - JETP 40, 678 (1975)].

[11]J. Larsson, L. Stenflo, and R. Tegeback, J. Plasma Phys. 16, 37 (1976).

[12]E. Valeo, C. Oberman, and F.W. Perkins, Phys. Rev. Lett. 28, 340 (1972); D.F. Dubois and M.V. Goldman, Phys. Rev. Lett. 28, 218 (1972).

[13]W.L. Kruer and E.J. Valeo, Phys. Fluids 16, 675 (1973); F.W. Perkins, C. Oberman, E.J. Valeo, J. Geophys. Res. 79, 1478 (1974).

[14]E. Ott, Phys. Fluids 18, 566 (1975).

[15]W. M. Hooke and S. Bernabei, Phys. Rev. Lett. 29, 1218 (1972); T. K. Chu, S. Bernabei, and R. W. Motley, Phys. Rev. Lett. 31, 211 (1973); R. P. H. Chang and M. Porkolab, Phys. Rev. Lett. 32, 1117 (1974).

[16]C. Oberman and G. Auer, Phys. Fluids 17, 1980 (1974).

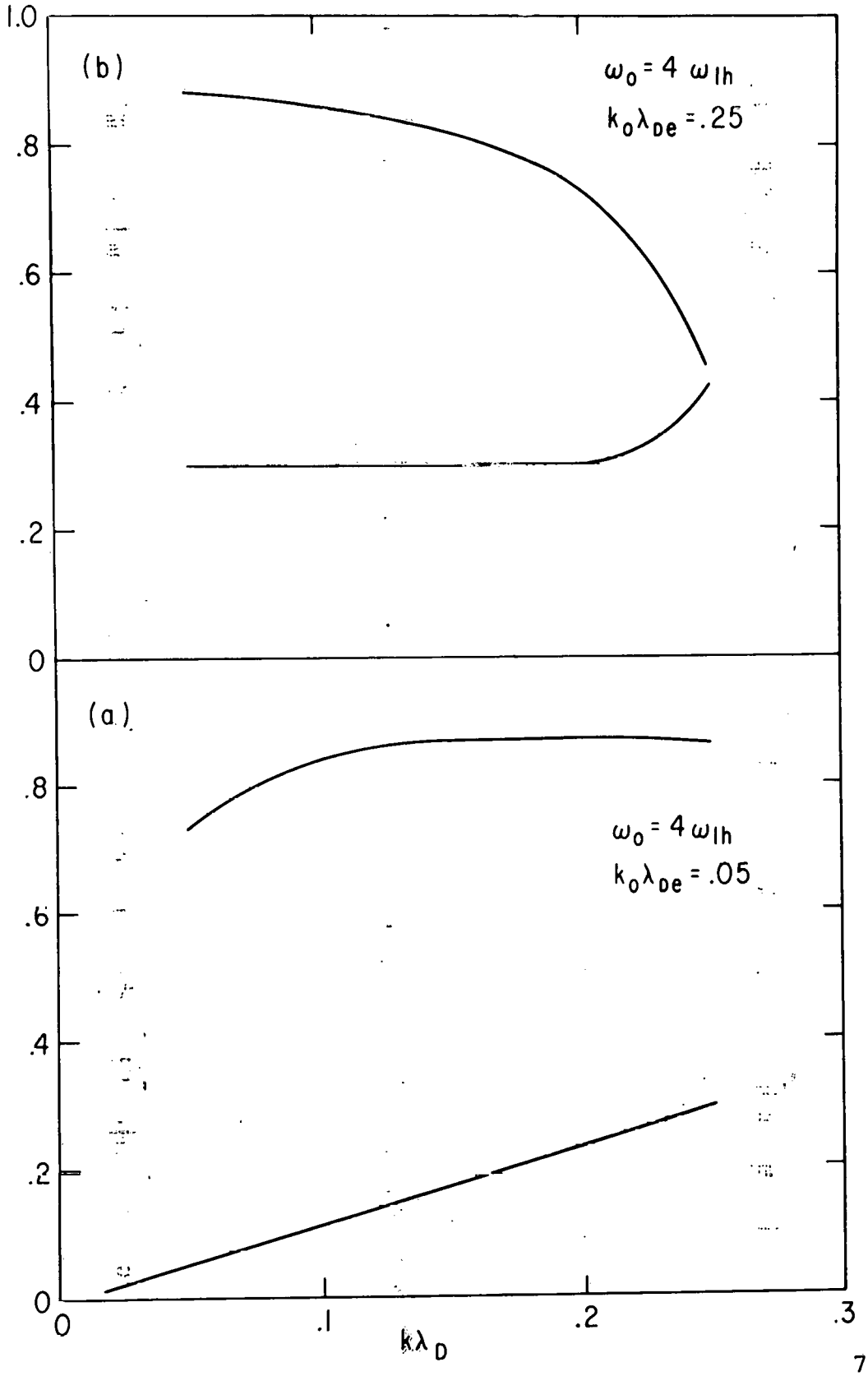

Fig. 1. The coupling function $B(\underset{\sim}{k}' - \underset{\sim}{k}', \omega_{\underset{\sim}{k}'} - \omega_{\underset{\sim}{k}})$ [see Eq. (10)] as a function of $k\lambda_{De}$ and maximized with respect to $k_{||}$ for pump frequency $\omega_o = 4\omega_{\ell h}$. The upper curve in each case is the maximum value of B and the lower curve is the frequency shift $(\omega_o - \omega_k)/\omega_{\ell h}$ that corresponds to this maximum value. (a) This case, $\omega_o = 4\omega_{\ell h}$ and $k_o\lambda_{De} = 0.05$, is similar to the results for a dipole pump where the maximum coupling is independent of wavenumber. (b) Short-wavelength pumps couple most effectively to long wavelengths.

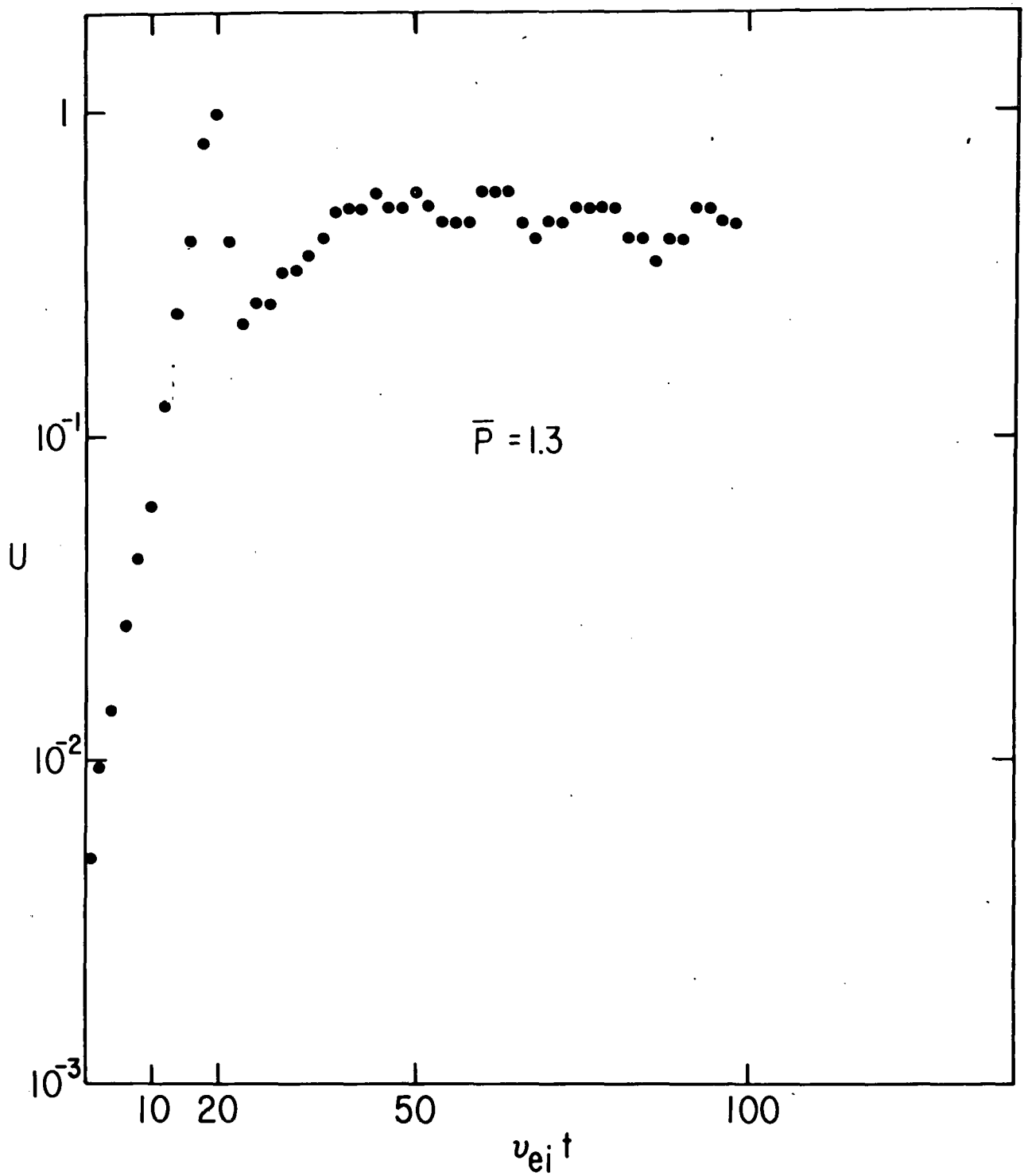

762204

Fig. 2. Total electrostatic energy as a function of time for $\omega_o = 1.42\omega_{\ell h}$, pump power relative to threshold power $\bar{P} = 1.3$, $T_e = T_i$, $\omega_{pe} = \omega_{ce}$, $\nu_e/\omega_{\ell h} = 10^{-6}$, and no convective loss ($\gamma^* = 0$).

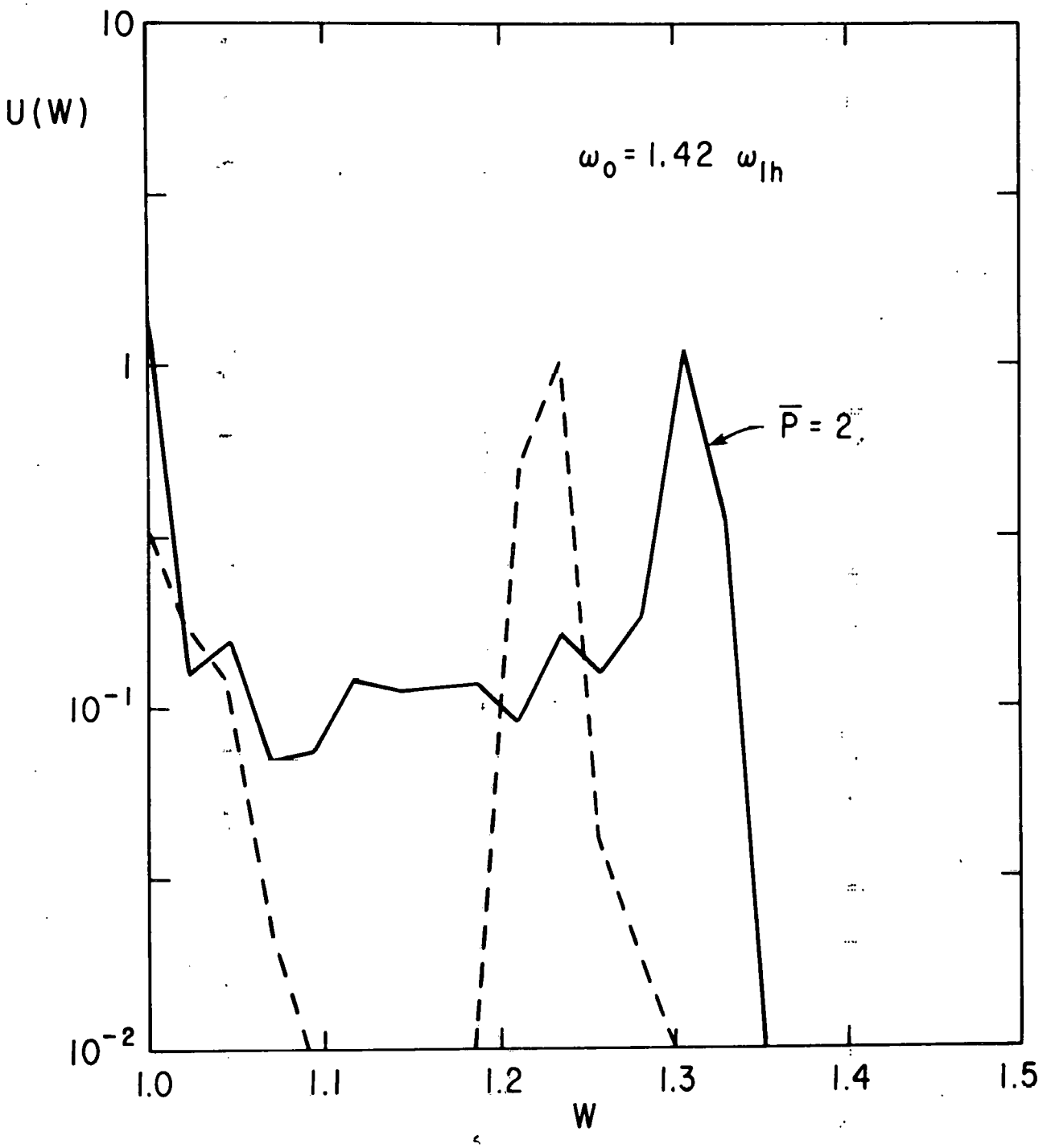

762208

Fig. 3. Total energy in decay waves U(W) per frequency interval normalized with respect to the pump energy. The dashed curve is the result for P = 1.3; the solid curve for P = 2.0. In both cases, $\omega_o = 1.42\omega_{\ell h}$, $T_e = T_i$, $\omega_{pe} = \omega_{ce}$, $\nu_e/\omega_{\ell h} = 10^{-6}$, and $\gamma^* = 0$.

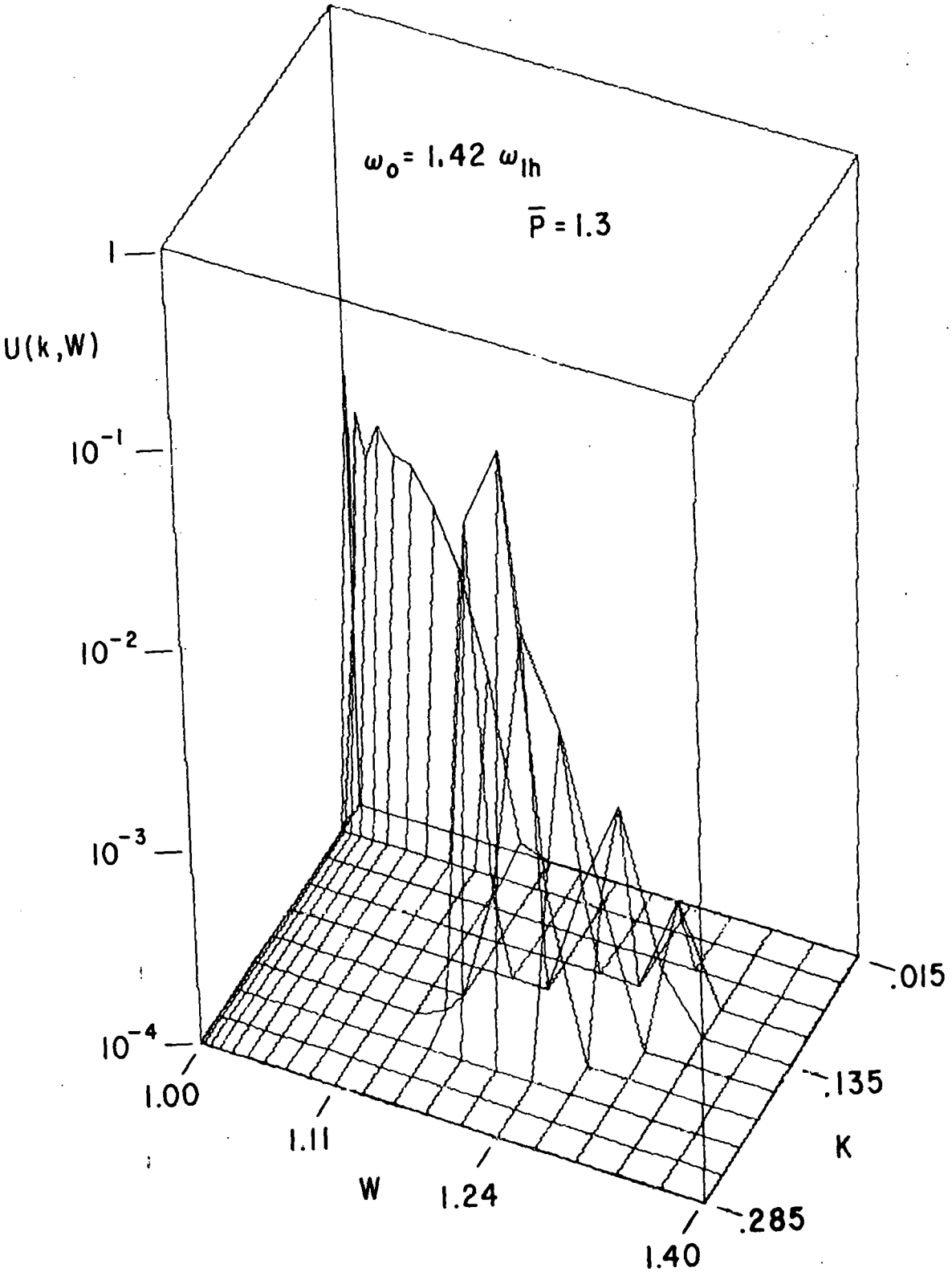

762211

Fig. 4. The energy in decay waves per wavenumber and frequency interval U(K,W) for P = 1.3, $\omega_o = 1.42\omega_{\ell h}$, $T_e = T_i$, $\omega_{pe} = \omega_{ce}$, $\nu_e/\omega_{\ell h} = 10^{-6}$, and $\gamma^* = 0$.

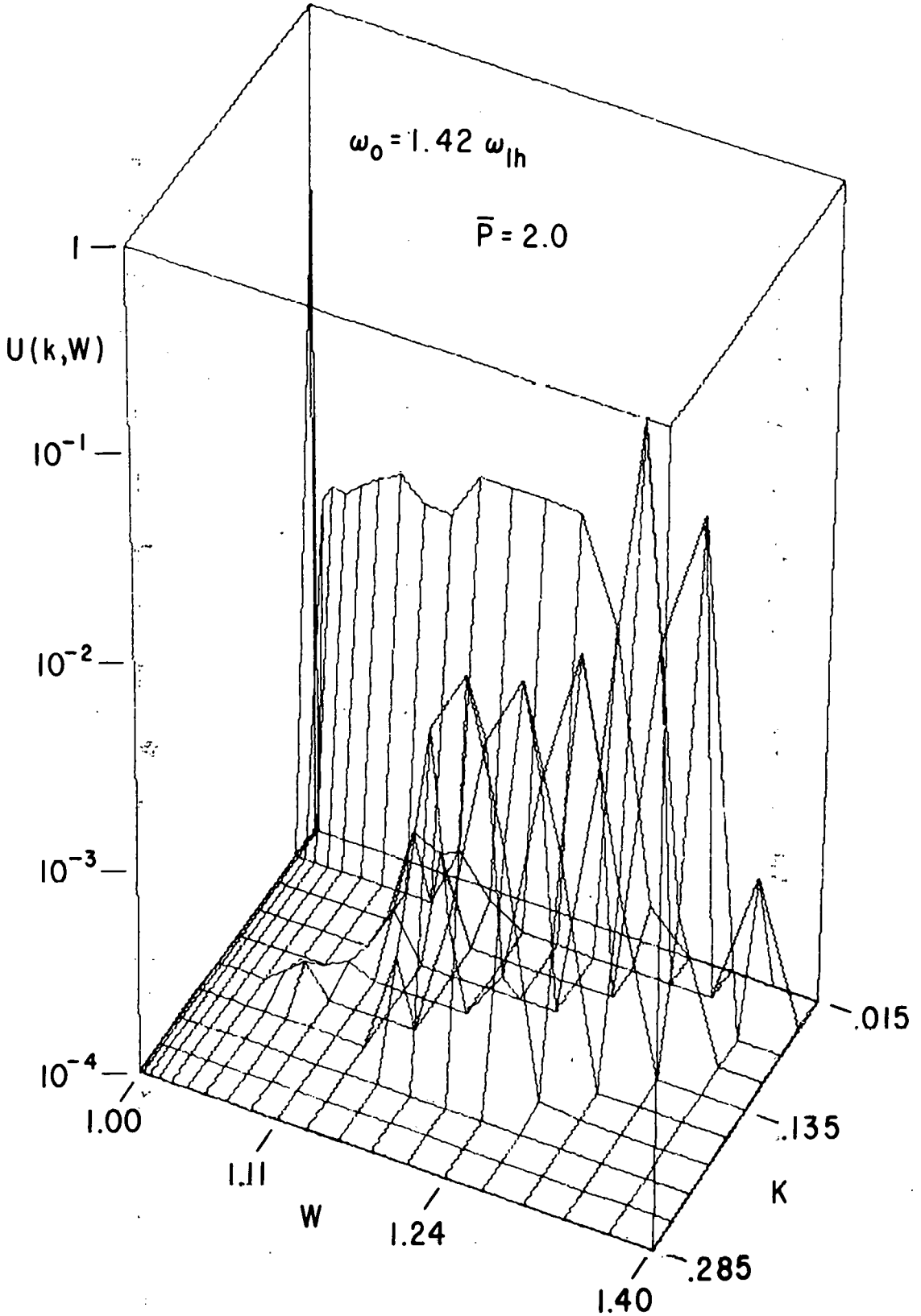

762212

Fig. 5. The energy in decay waves per wavenumber and frequency interval for P = 2.0, $\omega_o = 1.42\omega_{\ell h}$, $T_e = T_i$, $\omega_{pe} = \omega_{ce}$, $\nu_e/\omega_{\ell h} = 10^{-6}$, and $\gamma^* = 0$.

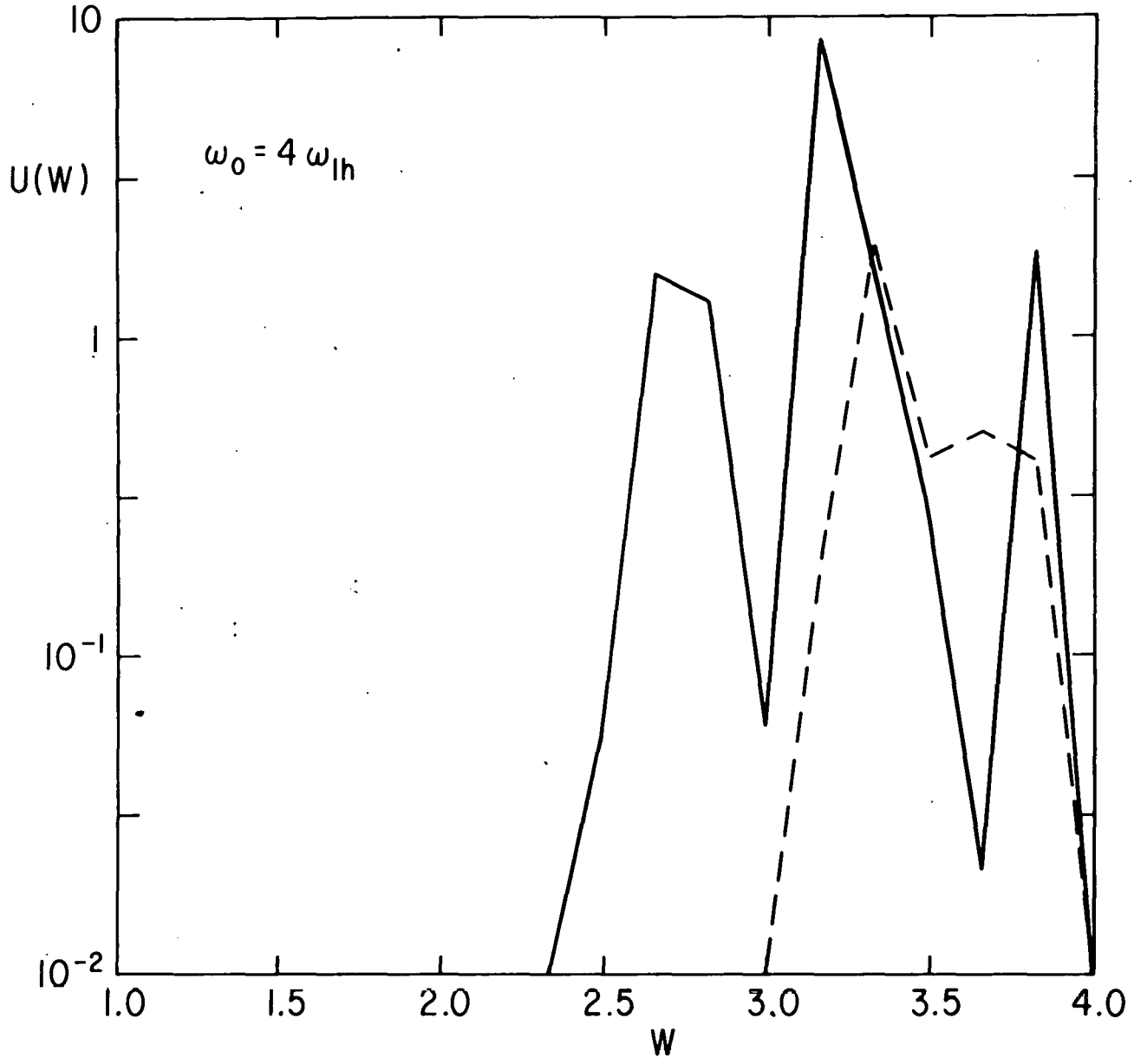

762209

Fig. 6. The energy in decay waves normalized to the pump energy as a function of frequency normalized to the lower hybrid frequency for $\omega_o = 4\omega_{\ell h}$ and P = 2 (dashed curve) and P = 4 (solid curve). In both cases, $T_e = T_i$, $\omega_{pe} << \omega_{ce}$, $\nu_e/\omega_{\ell h} = 2.10^{-5}$, and $\gamma^* = 0$.

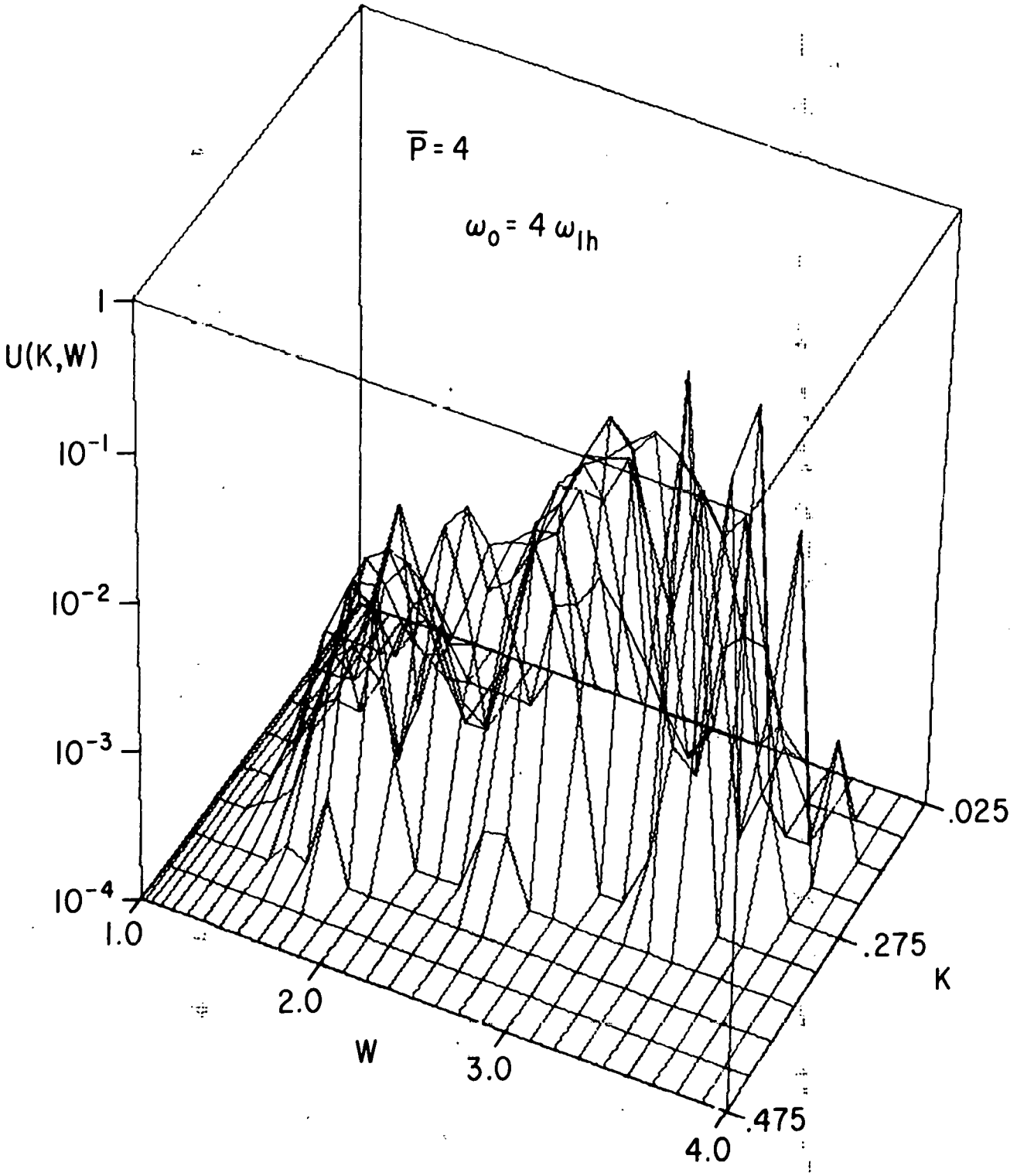

762214

Fig. 7. The energy in decay waves normalized to the pump energy per wavenumber and frequency interval for $\omega_o = 4\omega_{\ell h}$, P = 4, $T_e = T_i$, $\omega_{pe} << \omega_{ce}$, $\nu_e/\omega_{\ell h} = 2 \times 10^{-5}$, and $\gamma^* \neq 0$. Convection was included in this case. The minimum linear damping occurred for K ≃ 0.20.

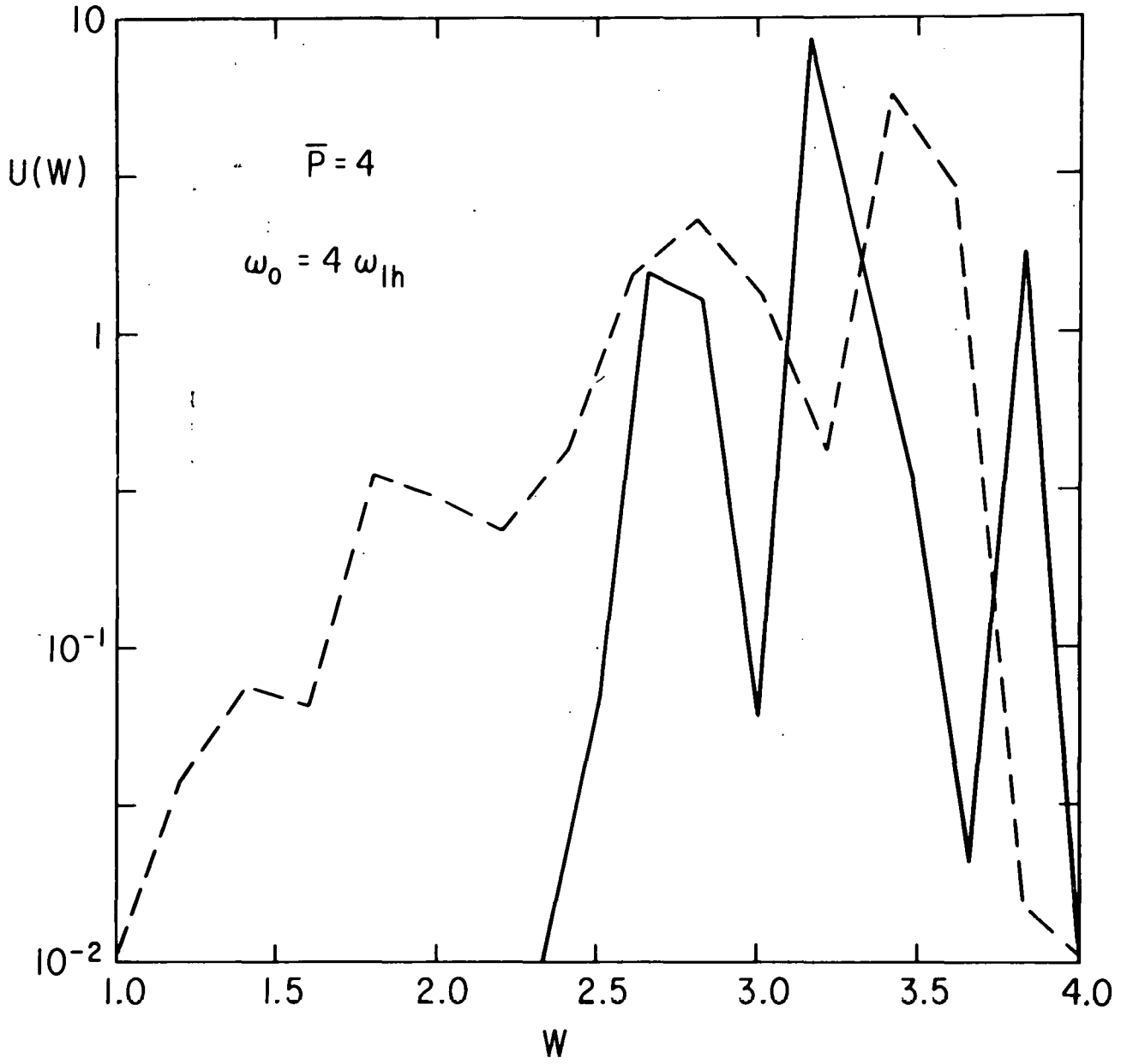

762210

Fig. 8. A comparison of the energy per frequency interval without convection (solid curve) and with convection (dashed curve) when $\omega_o = 4\omega_{\ell h}$, $P = 4$, $T_e = T_i$, $\omega_{pe} << \omega_{ce}$, $\nu_e/\omega_{\ell h} = 2 \times 10^{-5}$.

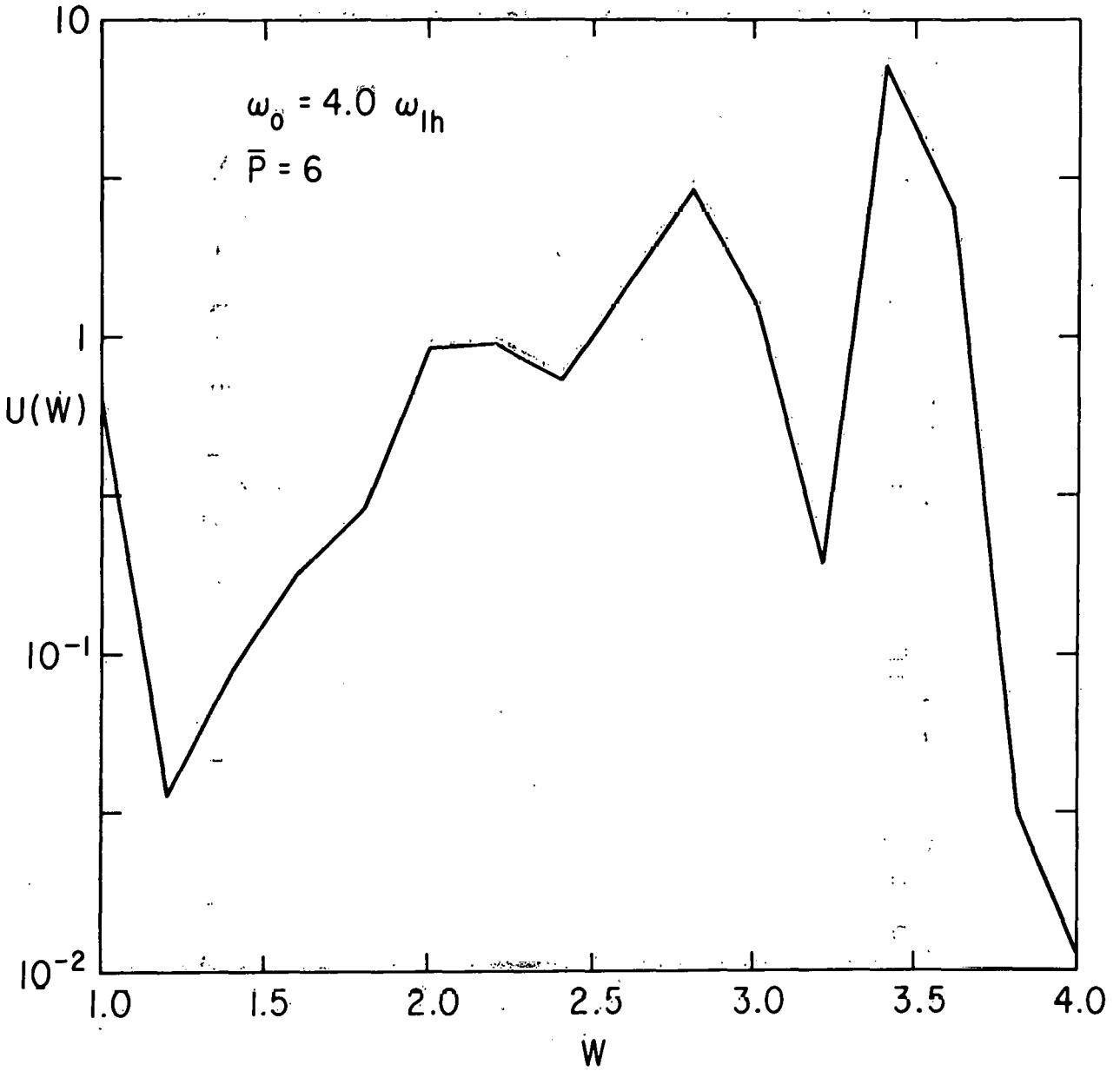

762207

Fig. 9. The decay wave energy per frequency interval for $\bar{P} = 6$ and $\omega_o = 4.0\omega_{\ell h}$ including convection. Note that energy appears to be accumulating in modes with frequency $\omega \doteq \omega_{\ell h}$. Other parameters are $T_e = T_i$, $\omega_{pe} \ll \omega_{ce}$, $\nu_e/\omega_{\ell h} = 2 \times 10^{-5}$.

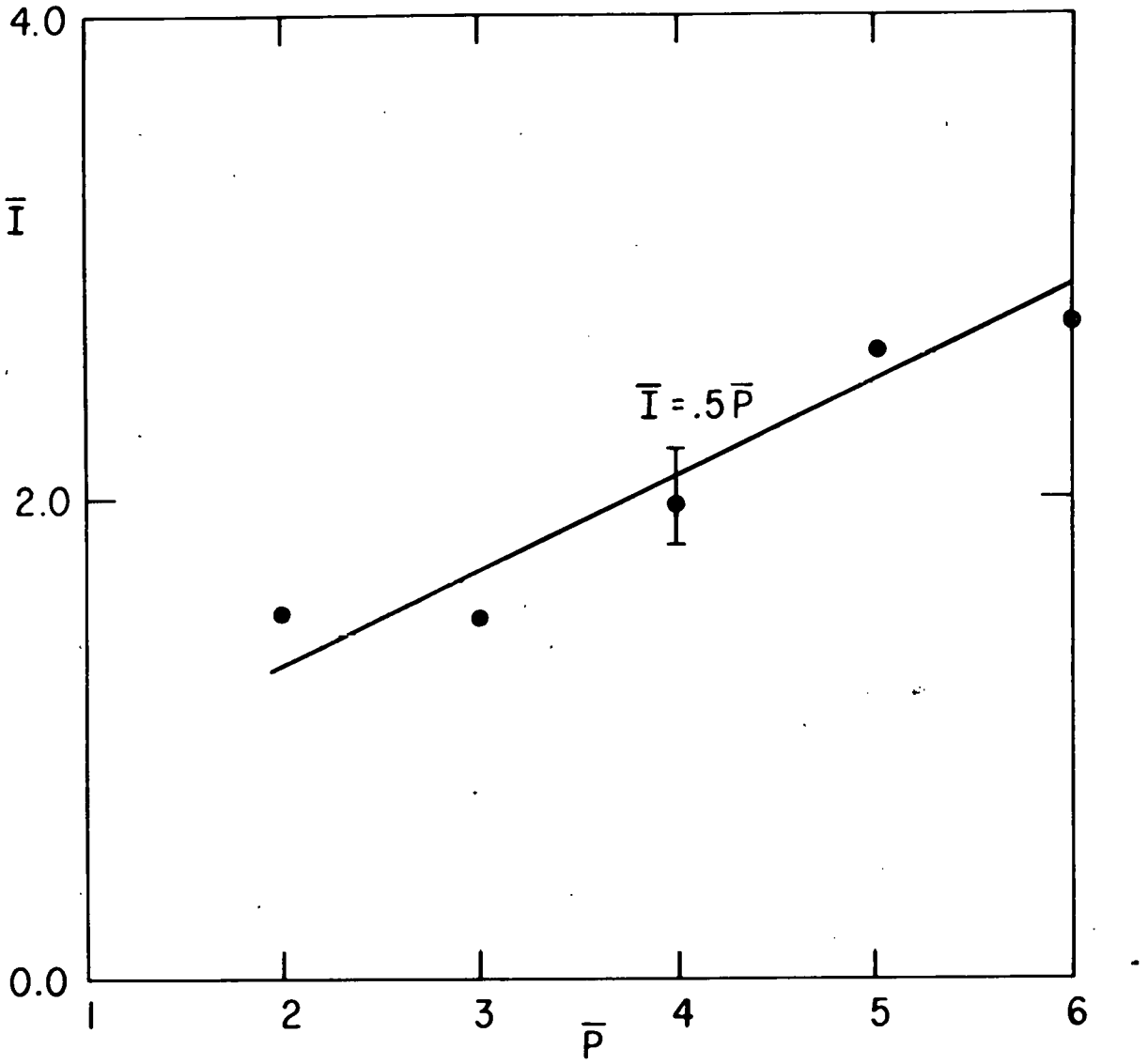

762205

Fig. 10. The total decay wave action normalized to the pump action, $\bar{I} = I/I_o$, as a function of pump power relative to threshold P for $\omega_o = 4\omega_{\ell h}$. Convective losses are included. Other parameters are $T_e = T_i$, $\omega_{pe} << \omega_{ce}$, and $\nu_e/\omega_{\ell h} = 2 \times 10^{-5}$.

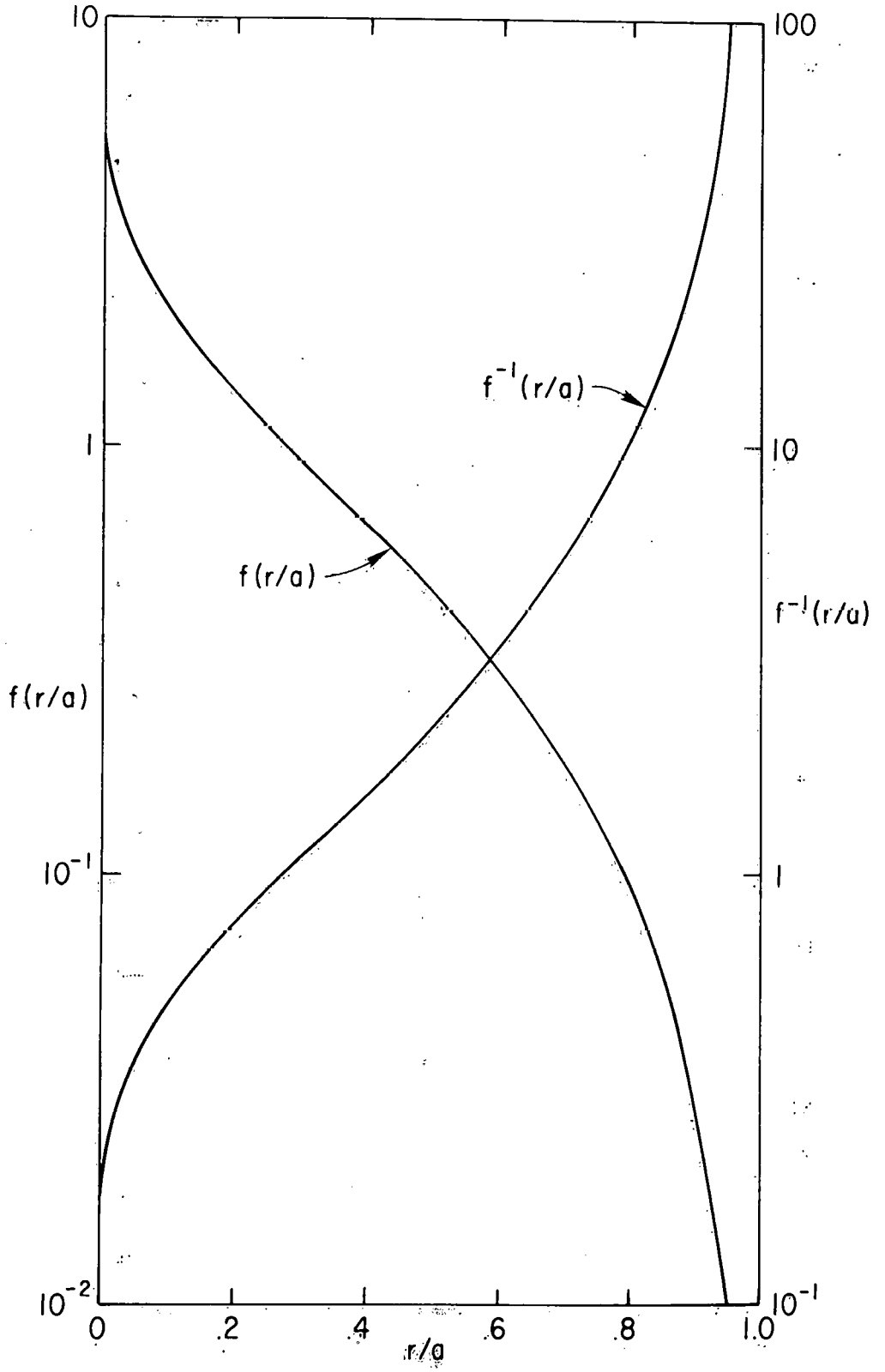

762247

Fig. 11. Graph of the functions f(r/a) and 1/f(r/a) defined in Eq. (39). The limiting power is related to f^{-1} via (37) and (40).

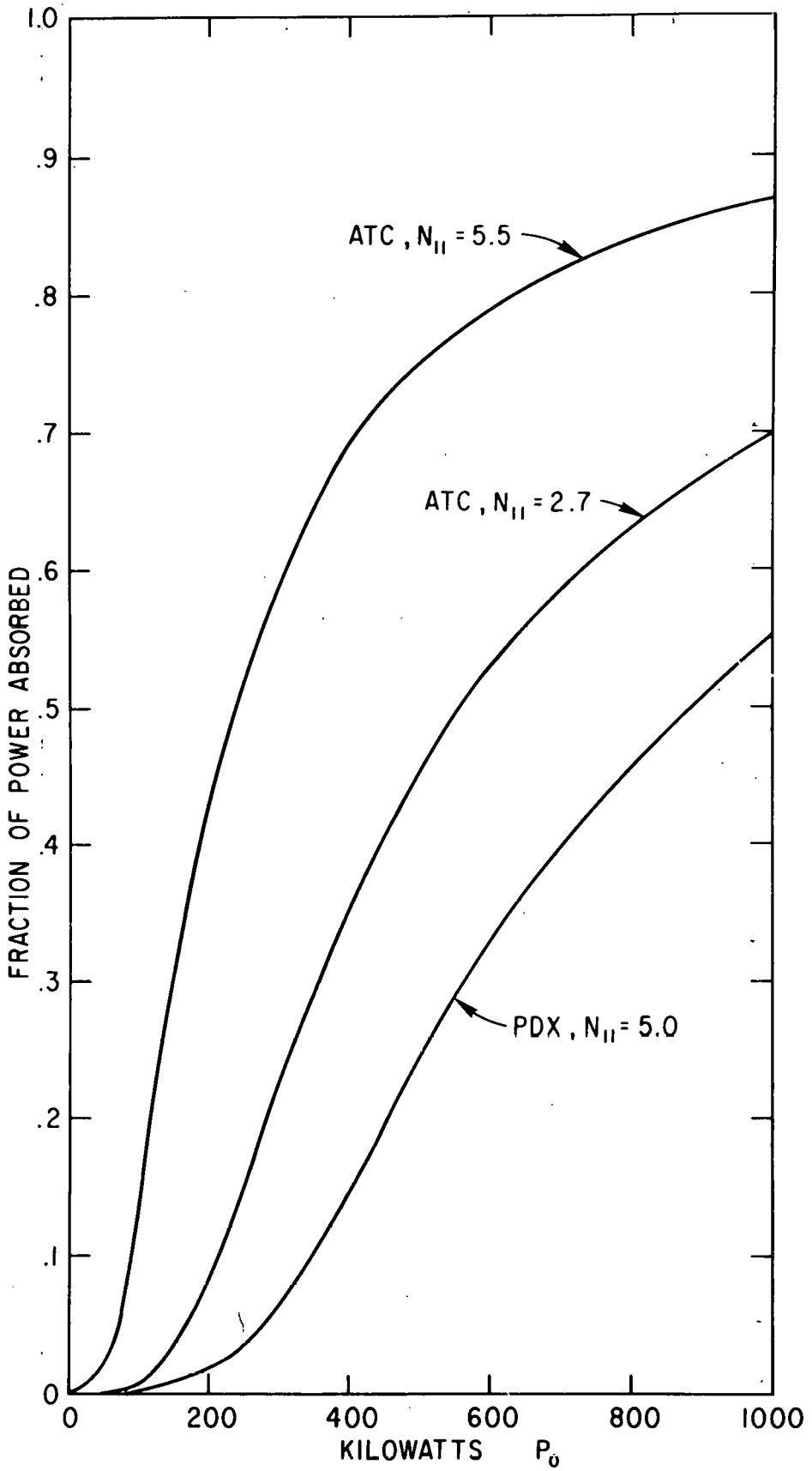

Fig. 12. The fraction of power absorbed as a function of the incident pump power P_o in kilowatts for typical Adiabatic Toroidal Compressor parameters and proposed Poloidal Divertor Experiment parameters. The $N_{||}$ label refers to the characteristic value of the parallel index of refraction of the pump. Other parameters are given in the text.